Genome analysis and elucidation of the biosynthetic pathway for the cRAS inhibitor rasfonin in Cephalotrichum gorgonifer

Andreas Schüller
University of Natural Resources and Life Sciences, Vienna (BOKU)
Lena Studt-Reinhold
University of Natural Resources and Life Sciences, Vienna (BOKU)
Harald Berger
University of Natural Resources and Life Sciences, Vienna (BOKU)
Lucia Silvestrini
University of Natural Resources and Life Sciences, Vienna (BOKU)
Roman Labuda
University of Veterinary Medicine Vienna
Ulrich Güldener
Technical University of Munich, TUM School of Life Sciences Weihenstephan
Markus Gorfer
AIT Austrian Institute of Technology GmbH
Markus Bacher
University of Natural Resources and Life Sciences Vienna (BOKU)
Maria Doppler
University of Natural Resources and Life Sciences
Erika Gasparotto
University of Natural Resources and Life Sciences, Vienna (BOKU)
Arianna Gattesco
University of Natural Resources and Life Sciences, Vienna (BOKU)
Michael Sulyok
University of Natural Resources and Life Sciences, Vienna (BOKU)
Joseph Strauss (joseph.strauss@boku.ac.at)
University of Natural Resources and Life Sciences, Vienna (BOKU)

Research Article

Keywords: Secondary metabolism, Cephalotrichum, Doratomyces NG_p51, rasfonin, transcriptome analysis, genome analysis, in silico retrosynthesis, biosynthetic gene cluster prediction, natural products discovery

Posted Date: November 11th, 2022

DOI: https://doi.org/10.21203/rs.3.rs-2250512/v1

Additional Declarations: No competing interests reported.

Version of Record: A version of this preprint was published at Fungal Biology and Biotechnology on June 24th, 2023. See the published version at https://doi.org/10.1186/s40694-023-00158-x.

Abstract

Background

Fungi are important sources for bioactive compounds that find their applications in many important sectors like in the pharma-, food- or agricultural industries. In an environmental monitoring project for fungi involved in soil nitrogen cycling we also isolated *Cephalotrichum gorgonifer* (strain NG_p51). In the course of strain characterization work we found that this strain is able to naturally produce high amounts of rasfonin, a polyketide inducing autophagy, apoptosis, necroptosis in human cell lines and shows anti-tumor activity in RAS-dependent cancer cells.

Results

In order to elucidate the biosynthetic pathway of rasfonin, the strain was genome sequenced, annotated, submitted to transcriptome analysis and genetic transformation was established. Biosynthetic gene cluster (BGC) prediction revealed the existence of 22 BGCs of which the majority was not expressed under our experimental conditions. In silico prediction revealed two BGCs with a suite of enzymes possibly involved in rasfonin biosynthesis. Experimental verification by gene-knock out of the key enzyme genes showed that one of the predicted BGCs is indeed responsible for rasfonin biosynthesis.

Conclusions

The results of this study lay the ground for molecular biology focused research in *Cephalotrichum gorgonifer*. Furthermore, strain engineering and heterologous expression of the rasfonin BGC is now possible which allow both the construction of rasfonin high producing strains and biosynthesis of rasfonin derivates for diverse applications.

Background

Fungi as producers of bioactive substances

Filamentous fungi have the potential to produce a countless number and huge diversity of bioactive substances, also called secondary metabolites (SMs). Those substances fulfil many different functions in the ecology and lifecycles of fungi. They are produced in response to certain developmental stages, metabolic or environmental conditions and stresses, like extreme temperatures (1), osmotic stress (2), UV-radiation (3), nutrient starvation (4, 5), in defence to other organisms such as competitors (6), mating partners (7) and during host-pathogen interactions as signalling molecules or virulence factors (8). SMs are thus molecules that are not essential for viability, but provide a selective advantage in specific situations during the life cycle of a fungal cell or colony. This is also the reason why almost all of these substances are only produced by fungi when a specific developmental, metabolic or environmental signal is present and genetically received. While some SMs can be potentially used as pharmaceuticals (i.e., Lovastatin (e.g., *Pleurotus ostreatus)* (9), Penicillin (*Penicillium sp.*) (10)), others can have detrimental effects as toxic food contaminant (i.e., aflatoxins (*Aspergillus flavus*) (11), fumonisins or deoxynivalenol (*Fusarium sp.*) (12, 13), etc.). Therefore, SMs are of major ecological, economical and medicinal importance.

Bioinformatic analysis suggests that fungal genomes typically hold the genetic information for dozens of so-called biosynthetic gene clusters (BGCs) that serve as blue prints for single SMs (14), and even more than 90 different BGCs in a single species have been reported (15). This genetic diversity gives rise to an enormous variety of SMs, even not considering the numerous intermediate products that are being produced on the way (16). This makes fungi sheer endless reservoirs for novel bioactive substances, given that there are estimated to be more than 5 million fungal species worldwide (17).

During a project that focused on the role of fungi within the nitrate assimilation process in agricultural soil, a community analysis was performed that elucidated the composition of species and the phylogenetic relationship of the genes responsible for nitrogen assimilation. For a few isolates, among them *Cephalotrichum gorgonifer* NG_p51 (previously classified as *Doratomyces sp.*), an unusual placement of the nitrate assimilation genes has been observed (18, 19). This led to the conclusion that there had to be an, until then, unknown way of acquisition of the complete nitrate assimilation cluster including the nitrate transporter, the nitrate reductase and the nitrite reductase by horizontal gene transfer. It was proposed that the cluster was transferred from a donor at the base of the Pezizomycotina to a recipient in the Microascales, to which *C. gorgonifer belongs* (20). Clustering of the three genes was retained, which

is otherwise unusual in the Sordariomycetes. These findings prompted us to investigate also possible acquisitions of BGCs coding for SMs from other fungi to *C.gorgonifer*.

It is well established that the reason for no expression of BGCs under standard laboratory conditions is chromatin-based silencing (21–25). We and others have thus used genetic or chemical chromatin modification to leverage the production of novel SMs in a number of fungi (e.g., treatment of *Doratomyces sp.* with the HDAC inhibitor valproic acid (26), deletion of a chromatin remodeler-encoding gene, *kdmB* in *Aspergillus nidulans* (27, 28), removal of the heterochromatic marks in *Fusarium fujikuroi* (29), etc.). For recent reviews on genetic and "chemogenetic" methods to active silence BGCs for SMs see (25) and (30). Using a medium throughput effort, we have tested hundreds of isolates from different environmental screening campaigns for their capacity to produce novel SMs upon chromatin activation. In the case of *C. gorgonifer* NG_p51, this led to the observation of bacterial growth inhibition and the discovery of several additionally produced compounds (26).

Further investigation in our in-house metabolite screening facility (31) revealed that *C. gorgonifer* is able to produce rasfonin, an SM initially isolated from *Talaromyces* strains and found to induce apoptosis in ras-dependent tumor cells (32–35). Although rasfonin has the potential of being a future pharmaceutical, the biosynthetic pathway is still not known. This, however, would greatly assist further research on this SM and facilitate the generation of rasfonin over-production strains for large scale applications. Therefore, we characterized *C. gorgonifer* NG_p51 in more detail on a genomics, transcriptomics and metabolomics level and established state-of-the-art molecular biology methods for this fungus. To elicit its putative chemical potential, we also conducted experiments to activate BGCs in *C. gorgonifer* NG_p51 via inhibition of chromatin active enzymes.

We report here the biosynthetic pathway for rasfonin in *C. gorgonifer* NG_p51. Furthermore, we established state-of-the-art molecular biology methods and performed various "omics" analysis for further strain and species characterization (i.e., genome analysis, BGC prediction, transcriptome analysis, morphological description, genetic transformation, CRISPR/Cas, …).

Results

Strain characterization of Cephalotrichum gorgonifer NG_p51

Ecology and taxonomy

We previously isolated the fungal strain NG_p51 and according to the former taxonomic positioning determined the genus of the strain by its ITS region as *Doratomyces* sp. (GenBank: HQ115716.1) (18). In the meantime, the genus *Cephalotrichum* (Microascaceae, Hypocreales) has been reorganized and now contains also species formerly affiliated to the genera *Doratomyces* and *Trichurus*. No sexual morphs have been observed. *C. gorgonifer* is frequently found in soil, decaying plant materials, dung and on wet cellulosic materials indoors. Occasionally it has also been isolated from human hair and respiratory samples. Their temperature optimum is around 25°C to 30°C but also growth at 37°C has been observed for several isolates. There are however no indications for human pathogenicity but data in this regard is scarce (36, 37).

We performed a phylogenetic analysis with ITS sequences (= Internal transcribed spacer regions of the rDNA and 5.8S region) of strain NG_p51 (GenBank No.: HQ115716.1), together with the *C. gorgonifer* (including the Ex-epitype of *C. gorgonifer*: *Trichurus spiralis* CBS 635.-78) and *Cephalotrichum telluricum* (i.e.: closest outgroup) dataset as published by Woudenberg et al. (37). The resulting phylogenetic tree shows that our strain clearly belongs to the species *C. gorgonifer* and that the *C. telluricum* species are clustered as an outgroup as expected (Fig. 1). We therefore designated the strain *C. gorgonifer* NG_p51.

Figure 1 Phylogenetic tree of Cehpalotrichum gorgonifer isolate NG_p51

A: Phylogenetic tree based on the ITS sequences of strain isolate NG_p51 together with several Cephalotrichum gorgonifer isolates and C. telluricum strains as closest. The tree entries follow following pattern: "accession number- genus and species-isolate identifier". The *phylogenetic analysis shows that strain isolate NG_p51 belongs to the species Cephalotrichum gorgonifer. The tree is drawn to scale, with branch lengths measured in the number of substitutions per site. The strain isolate (i.e. NG_p51) used for all experiments in this publication and the Ex-epitype are written in bold letters.*

Morphology of C. gorgonifer NG_p51:

Colonies of *C. gorgonifer* NG_p51 reach a diameter between 35–55 mm on oat meal agar (OA), potato carrot agar (PCA) and potato dextrose agar (PDA) after 14 days at 25°C. They effuse a dark greyish black (Fig. 2a) mycelium, consisting of nearly velutinous layer of synnemata which are 1–2 mm in length (Fig. 2b) and formed by aggregation of conidiophores (the annelophores). Numerous curled sterile setae are present alongside the fertile part of the synnemata (Fig. 2c-d) and conidia are borne from ampuliform annelids which appear smooth-walled and ovoidal to broadly ellipsoidal with truncate base and rounded apex, measuring 4–6 x 3.5-4.0 µm (Fig. 2e). Phenotypic traits of the strain NG_p51 (especially presence of undulate sterile setae, greyish color of conidia *en-masse* as well as their shape and dimensions) are in perfect concordance with the species concept of *C. gorgonifer* (Bainier) Sandoival-Denis, Gené & Guarro (36), in older literature also described under a name *Trichurus spiralis* Hasselbr. by Domsch et al. (38) and Ellis (39).

Additionally, the growth on malt extract agar plates (MEA) at 28°C, 30°C, 32.5°C, 35°C and 37°C showed that NG_p51 behaves as published for *C. gorgonifer* (36). In the observed range, optimal growth was at around 28°C. At 35°C, radial growth was strongly impaired while at 37°C radial growth was arrested. However, within the inoculation spot, spores at 37°C were germinating and mycelia density was increasing over the 4 days of incubation (Fig. 3)

Figure 3 Radial growth of C. gorgonifer NG_p51 on MEA petri dishes at different 5 temperatures after 4 days.

SM analysis of C. gorgonifer

Initial work with NG_p51 revealed that it is capable of suppressing growth of *Staphylococcus aureus* and two clinical methicillin resistant isolates of *S. aureus* when grown in the presence of the HDAC inhibitor valproic acid. Valproic acid treatment increased the production of seven antimicrobial compounds (cyclo-(l-proline-l-methionine), p-hydroxybenzaldehyde, cyclo-(phenylalanine-proline), indole-3-carboxylic acid, phenylacetic acid and indole-3-acetic acid) and also lead to the biosynthesis of an otherwise absent compound which was identified as phenyllactic acid (26). Also, rasfonin has been found in these screens, although the production of this bioactive compound was subsequently shown not to be dependent on valproic acid in the growth medium (31). Initial analysis of the production conditions revealed that this metabolite is produced on AMM liquid medium and detectable within 48 hours of incubation (Fig. 6). Although rasfonin is a well-known bioactive compound with potential applications in cancer treatment (32–35), its biosynthetic pathway remains unknown. To decipher its production pathway, we sequenced the genome and searched for the presence of BGCs potentially coding for rasfonin production.

Genome analysis and gene annotation:

Whole genome shotgun sequencing of *C. gorgonifer* was performed by 454 pyrosequencing yielding 1.78 Gb of raw sequence data which were assembled into 48 scaffolds of overall 35.9 Mb (49.4-fold coverage, N50 of 2.07 Mb). A total of 10,469 gene models were predicted using two different GeneMark gene predictors and manual validation. The annotated ORFs account for 43.8% of the genome. The overall GC content is 55%, while the average GC content of ORFs is 60.3%. Genome sequence data and annotation was deposited in the European Nucleotide Archive (ENA) at EMBL-EBI with the project number PRJEB15373 which can be accessed online at (40).

Annotation of biosynthetic gene clusters (BGCs):

Around 1 (41) to 25 genes (42) can be involved in the biosynthesis of single SMs. In most cases these genes are coregulated and in collinear vicinity to each other forming so-called BGCs (43). Genes within these clusters can code for proteins that are responsible for the biosynthesis of the compound-defining backbone (polyketide synthase (PKS), non-ribosomal peptide synthetase (NRPS), terpene synthase (TPS), …), the modification of the chemical backbone structure (e.g., cytochrome P 450, transferases, oxidoreductases, O-methyltransferases…), the regulation (global or cluster specific transcription factors (TFs)) of the cluster genes or for transport (delivery to compartments or export to surrounding media) (14, 44).

For BGC annotation, antiSMASH 6.0.1 for fungi (fungiSMASH) was used with standard parameters (45). The prediction algorithm for fungal BGCs assigned 308 genes to 24 putative BGCs. Six BGCs, showed homology to BGCs from other species with similarities ranging from 20–100% which are included in Table 1 with their respective references (Only the best scoring homolog BGC is shown). Similarity in this case is defined as “percentage of genes within the closest known compound that have a significant BLAST hit to genes within the current region” (taken from antiSMASH documentation (45)). In total, ten PKSs and one type3-PKS, three NRPS-PKS hybrids, five NRPSs, six NRPS-like proteins and three putative TSs could be assigned.

Expression analysis of candidate biosynthetic genes and whole genome transcriptome sequencing under different physiological conditions.

To obtain information about the genome wide differential expression pattern of BGC genes we cultivated the fungus under conditions of active growth in liquid shake cultures for 24 hours in Aspergillus minimal medium (AMM) and compared the expression pattern with cells in stationary phase after 48 hours of growth on the same medium. Of all 10469 annotated genes, 717 genes that were predicted not to be part of a secondary metabolism pathway by antiSMASH were up-regulated at 48h and 818 were down-regulated. From the 308 genes that are putatively involved in secondary metabolism, 39 were up-regulated at the 48-hour timepoint and 40 were down-regulated. The remaining 231 genes stayed unaffected. 8855 genes were not differentially regulated between the two timepoints which are 85% of the annotated genes.

The whole transcript-dataset can be retrieved from the additional materials (Additional_file_2.xlsx). The whole transcriptome was uploaded at NCBIs Gene Expression Omnibus (GEO) (46) under the accession number GSE217303

To estimate the transcriptional activity of BGCs under the chosen conditions of active growth versus stationary phase, we categorized the transcriptional status of the key-enzymes within a given BGC into three states (Table 1 Column Expression; Cat.). The expression of category 1 genes is not detectable or falls below the arbitrarily set threshold of biological relevance (see caption of Table 1) at both time-points (i.e. 14 of 29 genes). Category 2 genes (3 genes) are expressed only at one time point (i.e. either 24h or 48 hours) and the expression of category 3 genes (12 genes) is above the threshold at both 24h and 48 hours, although their expression levels may vary between the two time points (7 genes with at least a 2-fold difference between the time points). The individual expression levels, differential regulation between 24h and 48h and their respective transcriptional category of all predicted key-enzyme encoding genes can be retrieved from Table 1.

Table 1

Summary of BGCs of Cephalotrichumg gorgonifer NG_p51 as predicted by antiSMASH. Columns: ID: Cluster ID as assigned by antiSMASH; BB-gene(s): gene number of the key-enzyme encoding genes; type: type of key- enzyme; Range (genes): The predicted borders of the BGC with the total gene count in parenthesis; Expression: Expression of backbone genes at 24h and 48h are depicted as a 2-zone heatmap (weak expression | red –> blue |strong expression), based on their RPKM value. An arbitrary log-value of 1 was considered as a biologically relevant expression threshold under which, the expression was set to zero. The column "Δ" depicts the differential expression between 24-hour and 48-hour samples and is visually supported by a 3-zone heatmap (down-regulated @ 48h | blue –> white –> red | up-regulated @ 48h) with zero being the turning point. A significance value of $p < 0.05$ was applied as threshold which is indicated by an Asterix near the differential expression value. If the differential expression is higher than 2-fold, it is indicated with an additional "+". The Cat.: Expression Category (Cat1: Silent at 24h and 48h; Cat2: Expressed at either 24h or 48h (i.e. differentially expressed); Cat3 (Expressed at both 24h and 48h). Best scoring homolog BGCs in other species that were found by antiSMASH are also displayed together with their similarity in % and references.

ID	BB-gene(s)	Type	Expression (BB- gene)				Homologs (Species)	Similarity	Ref.
			24h	48h	Δ	Cat.			
1	DNG_00901	terpene	5.6	6.2	0.6	Cat3	-	-	-
2	DNG_01262	T1PKS	5.3	5.6	0.3	Cat3	naphtalene BGC (*Daldinia eschscholzii*)	33%	(47)
3	DNG_01539	T1PKS	1.7	3.7	2.0	Cat3	-	-	-
4	DNG_02059	T3PKS	4.9	6.1	1.2*,+	Cat3	-	-	-
5	DNG_02555	terpene	6.8	4.3	-2.5*,+	Cat3	-	-	-
6	DNG_02774	T1PKS	0.0	6.4	7.7*,+	Cat2	-	-	-
	DNG_02782	T1PKS	0.0	6.2	9.5*,+	Cat2		-	-
7	DNG_03072	T1PKS	0.0	0.0	-	Cat1	-	-	-
8	DNG_04293	NRPS	0.0	0.0	-	Cat1	-	-	-
	DNG_04303	T1PKS	0.0	0.0	-	Cat1			
9	DNG_04582	NRPS-T1PKS	0.0	0.0	-	Cat1	betaenone A – C (*Phoma betae*)	25%	(48)
10	DNG_04746	terpene	7.7	7.5	-0.1	Cat3	Squalestatin (*Aspergillus* sp.)	40%	(49)
11	DNG_06431	T1PKS	0.0	0.0	-	Cat1	-	-	-
12	DNG_07105	T1PKS	0.0	0.0	-	Cat1	-	-	-
	DNG_07107	T1PKS	0.0	0.0	-	Cat1			
13	DNG_07411	NRPS	2.1	2.7	0.6	Cat3	-	-	-
14	DNG_08044	NRPS	0.0	1.9	0.9	Cat2	phyllostictine A/B (*Phyllosticta cirsii*)	20%	(50)
	DNG_08052	NRPS-T1PKS	0.0	0.0	-	Cat1			
15	DNG_08262	NRPS-like	0.0	0.0	-	Cat1	-	-	-
16	DNG_08309	NRPS	5.4	1.4	-4.1*,+	Cat3	Dimethylcoprogen (*Alternaria alternate*)	100%	(51)
17	DNG_09028	NRPS-like	5.2	5.2	0.0	Cat3	-	-	-
18	DNG_09136	NRPS-like	0.0	0.0	-	Cat1	-	-	-
19	DNG_09754	NRPS	0.0	0.0	-	Cat1	-	-	-
20	DNG_09868	NRPS-like	5.0	1.6	-3.4*,+	Cat3	-	-	-

ID	BB-gene(s)	Type	Expression (BB- gene)				Homologs (Species)	Similarity	Ref.
			24h	48h	Δ	Cat.			
21	DNG_09951	NRPS-like	0.0	0.0	-	Cat1	-	-	-
22	DNG_10196	NRPS-like	7.3	5.6	-1.7*,+	Cat3	-	-	-
23	DNG_10230	NRPS-T1PKS	0.0	0.0	-	Cat1	cytochalasin E / K (*Aspergillus clavatus*)	23%	(52)
24	DNG_10425	T1PKS	0.0	0.0	-	Cat1	-	-	-

Prediction of the BGC responsible for rasfonin biosynthesis based on PKS domain structure.

Rasfonin (Fig. 4) is an α-pyrone-containing natural product composed of two distinct acetate-based polyketide (PK) chains. The PK chains are derived from the condensation of four and six acetyl-CoA subunits resulting in the formation of a partially reduced and di- and trimethylated tetra- and hexaketide, respectively, that are further modified (hydroxylation) and finally linked via an ester bound. These chemical features suggest the involvement of two highly-reducing PKS (HR-PKSs) containing, in addition to the essential acyltransferase (AT), ketoacyl-synthase (KS), and acyl carrier protein (ACP) domains, domains involved in the reduction of the growing PK chain, i.e., a ketoreductase (KR), a dehydratase (DH) and an enoylreductase (ER). Next to this, the methyl groups at C6, C8, C10, and C4', C6', suggest the presence of an intrinsic C-methyltransferase (MT) domain that functions in the transfer of a methyl group from S-adenosylmethionine (SAM) to a β-ketoacyl-ACP substrate for both involved PKSs.

We thus screened the genome sequence of *C. gorgonifer* for the presence of predicted PKS- encoding genes that harbour a domain composition putatively fitting the enzymatic functions necessary for rasfonin biosynthesis. Bioinformatic analysis of the 14 PKSs present in the *C. gorgonifer* genome revealed that seven HR-PKSs harbour the necessary domain architecture (Fig. 5A). Only two BGCs contain two HR-PKSs in close proximity to each other namely BGC 6 (Table 1 ID 1) with the combination of [CgPKS4 + CgPKS5] (Fig. 5A) and BGC 12 (Table 1 ID 12) with the combination [CgPKS10 + CgPKS11] (Fig. 5A). Both also encode a putative transferase, i.e., DNG_02776 and DNG_07106, respectively. To further define which of the two BGCs is involved in rasfonin biosynthesis, we questioned our transcriptome data set and found that only the BGC with the HR-PKS pair *CgPKS4* and *CgPKS5* (Fig. 5A; Table 1 ID 6) showed expression at 48 hours. The other candidate pair *CgPKS10* and *CgPKS11* (Fig. 5A; Table 1 - ID 12) were not expressed at any tested condition.

Next, we set out to analyse the extension of the CgPKS4/ CgPKS5 BGC. Our transcriptome data showed a clear coregulation in expression of the genes that are positioned between *CgPKS4* and *CgPKS5*. No transcription was observed 24 hours post inoculation (hpi) while expression of all genes was significantly upregulated 48 hpi. The genes upstream of CgPKS4 and downstream of CgPKS5 were not coregulated (Fig. 5B). The GO annotations of adjacent genes do not suggest that they are involved in the synthesis of rasfonin. Thus, the BGC likely spans nine genes, i.e., DNG_02774-DNG_02782. To evaluate the contribution of the putative CgPKS4/ CgPKS5 BGC to rasfonin biosynthesis, one of the PKS-encoding genes, *CgPKS4*, was arbitrarily chosen for targeted gene disruption.

Figure 5 A *Domain organization was analysed using the NCBI Conserved Domain (36), InterPro (37), SBSPKSv2 (38); and the PKS/NRPS Analysis Web-site (39). KS (red), keto synthase; AT (yellow), acyltransferase; DH (pink), dehydratase; MT (blue) C-methyltransferase; ER (grey) enoylreductase; KR (violet), ketoreductase; ACP (green), acyl carrier protein; cAT (orange), carnitine acyltransferase; Chalcone/stilbene_synt_N (lime-green): Chalcone/stilbene synthase N-terminal; Chalcone/stilbene_synt_C (dark-cyan): Chalcone/stilbene synthase C-terminal. The proposed PKS names are listed together with their gene number and length. The transcriptional activity at 24h or 48 hours ins indicated as "-" (No transcription at given timepoint) or "+" (transcription at given timepoint). The two PKS encoding genes that are proposed to be involved in the rasfonin synthesis (i.e. CgPKS4 and CgPKS5) are highlighted by a red box* B *The proposed BGC for rasfonin biosynthesis is depicted with transcript at 24h and 48h timepoint (shake flask culture, AMM). The BGC borders are depicted in red and were assigned based on the coregulation of genes. Proposed BGC gene names (rsf1 to rsf9) are depicted above gene illustrations.*

Experimental Verification Of The Bgc Involved In Rasfonin Biosynthesis

The standard method to prove the involvement of a respective candidate gene in SM biosynthesis is deletion of the coding region in the genome, accompanied by the loss of product formation. However, so far *Cephalotrichum* sp. have not yet been genetically modified and

used for reverse genetics approaches. Therefore, a transformation method had to be established with the aim to disrupt or mutate *CgPKS4* and show by chemical analysis that rasfonin is not produced any longer in the transformed strain. To maximize the chance obtaining *CgPKS4* mutations by transformation, three different approaches were selected, i.e., a Cas9 approach (Strain Cg-Cas9-02774-1), an agrobacterium-mediated transformation approach (Strain Cg-At-02774-1) and also a homology directed repair (HDR) approach via protoplast-mediated transformation of a linear fragment (Strain Cg-HDR-02774-1) (53, 54). All three transformation methods were successfully implemented in our *C. gorgonifer* strain NG_p51. Cas9 and the HDR transformations were performed on kryo-stocks of *C. gorgonifer* protoplasts (see material and methods section).

Disruption of *CgPKS4* by Cas9 resulted in the strain Cg-Cas9-02774-1. Sequencing of the locus revealed a 640 bp deletion ranging from base pair 269 (i.e.: sgRNA annealing site) to base pair 908 of the coding sequence (CDS), a mutation that additionally leads to a frameshift within the remaining CDS of the gene (Sequence at Cas9- restriction site: 5'- ACCAATGCACCCGGT | 640 bp deletion | GTTCGACCACCGCGC – 3') (see Additional_file_3.gbk).

The *A. tumefaciens* mediated mutation resulted in the transformant Cg-At-02774-1 that has the first 2300 base pairs of *CgPKS4* (DNG_02774) replaced with the hygromycin resistance cassette (hph), again resulting in a frameshift within the CDS. The 5'-end homology region spans 1200 base-pairs upstream of the start codon (i.e. promoter region) and the 3'- homology region spans 1500 base-pairs downstream of the exchanged fragment (i.e. first 2300 base pairs of the gene body) (see Additional_file_3.gbk).

The transformant Cg-HDR-02774-1 resulted from the HDR-directed approach. Here, the same replacement cassette was used as for the agrobacterium transformation (i.e., PCR product from the "HDR-Fragment" primer pair with template pAt-DNG02774; Additional_file_1.pdf Table S 1). Both strains (i.e., Cg-At-02774-1 and Cg-HDR-02774-1) were PCR tested for the successful gene replacement event (see Additional_file_1.pdf Figure S1; Additional_file_3.gbk))

To test if the mutated target gene is responsible for the biosynthesis of rasfonin, the transformants and the recipient strain NG_p51 were cultivated in parallel. The fungal colonies (mycelia + agar media) were extracted, and extracts were analysed by high performance liquid chromatography (HPLC) for the presence of rasfonin. None of the three tested mutants showed any detectable amounts of rasfonin (Figure 6C, left) when compared to the wildtype NG_p51 (Figure 6B, left). A 25 µg/mL rasfonin solution produced in our laboratory and verified by NMR (see materials and methods) served as analytical standard (Figure 6A). Next to this, we spiked the wildtype sample with our standard thereby unequivocally proofing that the peak in the wildtype chromatogram indeed is rasfonin (Figure 6B and C, right), and that rasfonin is missing in our *CgPKS4* mutants. To verify that not even trace amounts of rasfonin are produced that are not detected by our HPLC method, we subjected an extract from the Cg-Cas9-02774-1 strain to liquid chromatography-high resolution mass spectrometry (LC-HRMS). The results of this analysis *Figure 6 HPLC analysis of rasfonin between a 25 µg/mL rasfonin standard (green*, A*), the wildtype isolate NG_p51 (blue*, B left*) and the CgPKS4 knockout strain NG_p51ΔCgPKS4 (orange*, C left*). All 3 knockout strains and all replicates showed the same absence of rasfonin, but only one is shown here. Spiked samples are shown on the right panel and are indicated by a green peak (NG_p51*, B right; *NG_p51ΔCgPKS4*, C right*). The retention times in minutes are shown next to the peaks.*

showed no detectable amounts of rasfonin in the mutant strains (Additional_file_1.pdf Figure S2). This verifies that CgPKS4 (from now on referred to as Rsf1) is indeed directly involved in the biosynthesis of rasfonin in *C. gorgonifer* NG_p51.

Next to *CgPKS4* (*rsf1*), eight genes are coregulated under rasfonin-inducing conditions including a second PKS-encoding gene *CgPKS5* located at the end of the putative BGC. Thus, we propose that the BGC involved in rasfonin biosynthesis stretches between *CgPKS4* and *CgPKS5*, and comprises overall nine genes, *rsf1* to *rsf9* (Fig. 5B). Next to the PKSs, the BGC encodes three putative cytochrome p450s (DNG_02775: *rsf*2; DNG_02779: *rsf*6; DNG_02781: *rsf*8), a putative O-acyltransferase (DNG_02776: *rsf*3), a Major facilitator family1 (MFS1) transporter (DNG_02777: *rsf*4), one FSH domain-containing protein (DNG_02778: *rsf*5) as well as one uncharacterized protein (DNG_02780: *rsf7*).

Discussion

Rasfonin carries the potential of an anti-cancer pharmaceutical as it is active against several tumour types. Several studies found that rasfonin suppresses proliferation of pancreatic cancer cells with mutated K-ras which is an important oncogene affected in many cancer types. In K-ras mutated cells rasfonin showed stronger activity compared to cells with wild-type K-ras. The substance also reduced clone formation, invasion and migration of cells with mutated K-ras. Although the exact mechanism is unknown, it was observed that rasfonin strongly downregulates Ras activity and (directly or indirectly) reduces the expression of Son of sevenless (Sos1), a nucleotide exchange factor which is involved in RAS activation (34). In renal cancer cells, rasfonin promotes cell apoptosis and autophagy in connection with

the protein Akt (protein Kinase B) which is a frequently activated (i.e., phosphorylated) oncoprotein in tumour cells (33). In another study, a similar effect against clonal formation and migration of osteosarcoma 143B cells was also observed and autophagy was promoted (35). Another recent study with rasfonin found a connection between rasfonin induced caspase-dependent apoptosis and autophagy in ACHN cells (renal adenocarcinoma cell line) and the RPTOR and RICTOR proteins. While RPTOR seems to play a role in the rasfonin-induced apoptosis pathway, RICOTR is important for autophagy triggered by rasfonin (32). In a new study, Hou and colleagues found a functional link between rasfonin activity and necroptosis. Rasfonin enhanced Grb2 binding to a receptor-interacting kinase (RIP1), which plays a critical role in regulating programmed necrosis. These data suggest that Grb2 actively participates in rasfonin-induced necroptosis by interacting with components of the necrosome and mediating their expression. In summary, at the actual stage of knowledge, rasfonin seems mainly to trigger apoptosis and necroptosis through the activation of cellular pathways.

In fungi, the true physiological or ecological function of rasfonin remains obscure. No strong antimicrobial activity has been detected so far. Available data from experiments with cancer cell lines suggest a modulation of Ras-signalling pathways by rasfonin, which can suppress proliferation of certain cell lines (34). As a colonizer of cellulosic plant litter, *C. gorgonifer* would encounter numerous other eukaryotes, where alterations of their developmental program through modulation of Ras signalling could be potentially advantageous for the producing organism. However, other eukaryotic cells tested by us, such as *Saccharomyces cerevisiae*, seem highly resistant to this compound (our unpublished preliminary observations). The availability of KO strains without detectable rasfonin production will allow to test hypotheses on rasfonin function in the natural environment.

An interesting preliminary observation of our study was that the metabolite does not seem to be actively exported into the surrounding of the cell but stays within or attached to the mycelium in a fungal culture (unpublished preliminary observation). Although there is an expressed gene within the BGC that codes for a transporter, computational analysis of the predicted protein sequence by MULocDeep suggests that the transporter is targeted to a lysosome like membrane (55). This indicates that an intermediate or the final compound is stored within extra compartments like it is the case with fungal toxisomes (56, 57). Of course, some exporter, encoded by a gene residing externally of the rasfonin BGC, might be responsible for export, but this topic needs further investigation.

The biosynthesis of rasfonin is coordinated by two highly-reducing iterative type I PKSs. In general, two scenarios are possible that may yield rasfonin. In a first scenario one PKS generates a PK chain that serves as a starter unit and may be passed on to the second PKS for further extension. This mechanism has been proposed for zearalenone in *F. graminearum* (58), T-toxin in *Cochliobolus heterostrophus* (59), asperfuranone in *A. nidulans* (60) or botcinic acid in *Botrytis cinerea* (61). In a second scenario two PKSs are involved in the assembly of two distinct PK chains that are subsequently linked via an ester bond catalyzed by an acyltransferase encoded within the same BGC as it has been shown for lovastatin in *Aspergillus terreus* (62), and the related compactin in *Penicillium citrinum* (63). Noteworthy, in rare cases one PKS is involved in the assembly of two distinct PK chains as it has been recently shown for gregatin A in *Penicillium* sp. Sh 18 (64), or fusamarin in *Fusarium mangiferae* (65), and which is likely also true for fujikurin in *Fusarium fujikuroi* (66, 67). However, given the cluster architecture and co-regulation as well as the presence of two HR-PKS- and one putative transferase-encoding genes in the rasfonin BGC, DNG_02776 (*rsf3*), we propose the following route for rasfonin biosynthesis (Fig. 7): One HR-PKS, Rsf1 (CgPKS4) or Rsf9 (CgPKS5), is involved in the programmed assembly of the partially reduced 6,8,10-trimethylated hexaketide (1) by successive condensations of acetyl-CoA with 5 malonyl units, while the other assembles the 4',6'-dimethylated tetraketide (4). Noteworthy, none of the HR-PKSs harbors a release domain, but the presence of Rsf5, a predicted thioesterase (TE) with similarity to LovG from the lovastatin cluster (68), suggests that Rsf5 may function in the release of the hexaketide. Similar *trans*-TEs have been shown to facilitate off-loading in the case of fusarielin biosynthesis in *F. graminearum* (69), and fusamarin biosynthesis in *Fusarium mangiferae* (65). The PK chain may be released either by TE-mediated hydrolysis followed by the spontaneous intramolecular cyclization accompanied by dehydration yielding **2**, or the cyclization happens directly through TE-catalysed pyrone formation as it has been shown for the TE-domain of CTB1 involved in cercosporin biosynthesis in *Cercospora* sp. (70). **2** is then further modified to yield **3** by hydrogenation and subsequent hydroxylation of C4. The latter step is likely catalysed by one of the cytochrome p450s encoded within the BGC, Rsf2, Rsf6 or Rsf8. Next, Rsf3, encoding a putative O-acyltransferase with similarity to LovD (71) captures **4**, followed by the transacylation of **3** resulting in the formation of **5**, that is further hydroxylated at C8' and C10' likely catalyzed by one or both of the remaining cytochrome p450s encoded in the BGC, yielding the final product rasfonin (6).

Noteworthy, elucidation of the pathway was facilitated in this work by the availability of the whole genome and a genome-wide transcriptome along with a knowledge-based prediction of enzymatic domains which are known to synthesize similar molecules. But all this prediction work in the end needs experimental verification by targeted inactivation of the proposed biosynthetic gene. For non-model fungi, the transformation-mediated inactivation of a target genes is often not trivial. Our strategy was to follow three well-known strategies to reach that goal with a high probability of success. But still, some modifications of standard protocols were necessary. Here,

we developed a modified version of common protoplastation protocols to ensure a cost- and time efficient method. The possibility to use kryo-stocks significantly increases the speed and flexibility of transformation experiments. As different fungi will need different conditions during protoplastation and post-transformation regeneration, we want to highlight a publication by Wu and co-workers (72) which compares the impact of different buffer compositions and conditions on protoplastation and regeneration efficiency. The publication assisted in the development of the protoplastation protocol for *C. gorgonifer* and will surely also be of use in case of establishment of other fungal species for the laboratory environment.

Conclusions

This work provided the tools and methods for working efficiently with the rasfonin producing strain *Cephalotrichum gorgonifer NG_p51* in a laboratory environment. Thorough characterization and analysis in form of genome analysis, transcriptomics, phylogenetic analysis and morphology have been conducted which provide substantial information for further research. The elucidation of the BGC that is responsible for the biosynthesis of rasfonin enables strain and pathway engineering which could facilitate the development and high yield production of this putative pharmaceutically relevant compound. The establishment of three different transformation methods and the development of an adapted protocol for protoplast and protoplast-kryo stock preparation of *C. gorgonifer* NG_p51 significantly speeds up molecular genetics work with this fungus and will also help with establishing such methods in other fungal species. This will hopefully increase the pool of species that can be deployed in a laboratory environment and therefore promote the research on so far unknown novel BGCs.

Materials And Methods

Phylogenetic tree: Evolutionary analysis by Maximum Likelihood method:

ITS sequences (For accession numbers see Fig. 1) were aligned with the program MEGAX: Molecular Evolutionary Genetics Analysis across computing platforms (Version 10.2.6) (73) with the ClustalW algorithm (standard parameters) (74). After alignment, sequences were trimmed to equal length for the construction of the phylogenetic tree.

The tree with the highest log likelihood (-808.77) is shown. The percentage of trees in which the associated taxa clustered together is shown next to the branches. Initial tree(s) for the heuristic search were obtained automatically by applying Neighbor-Join and BioNJ algorithms to a matrix of pairwise distances estimated using the Tamura-Nei model (75), and then selecting the topology with superior log likelihood value. This analysis involved 21 nucleotide sequences. There was a total of 557 positions in the final dataset. Evolutionary analyses were also conducted in MEGA X. Bootstrapping was performed 500 times.

Morphological analysis of strain NG_p51

For phenotypic characterization, the strain *Cephalotrichum gorgonifer* NG_p51 was transferred on Potato Dextrose Agar (PDA, Fluka), Malt Extract Agar (MEA, Merck) and Oatmeal Agar (OA) as described by (76) and incubated for 14 days in the dark at 25°C. For comparative description of the macroscopic and microscopic characteristics, OA was used according to (36), and additionally compared to (39) and (38) where the fungus is described and illustrated under the name *Trichurus spiralis* (current name: *Cephalotrichum gorgonifer* (36)). The photomicrographs were taken using a Motic BA 310 microscope with Motic Image Plus 3.0 software. Lactophenol blue was used as a mounting medium for microphotography. Photographs of the colonies were taken with a Sony DSC-RX100.

Growth phenotype at different temperatures

For determining the growth morphology under different temperatures, spores of strain NG_p51 were grown by plating them from kyro-stocks (50% Tween-20 0.1% spore suspension and 50% glycerol 50% (w/v)) on MEA plates at 30°C for 4 days. Spores were harvested by scraping off the agar with a spatula and 0.1% Tween solution. The spore suspension was then filtered through glass wool filled tips and a 1/1000 dilution was prepared (3 subsequent 1/100 dilutions; 100µL spore solution and 900 µL Tween 0.1%) were then counted in a counting chamber (Neubauer improved; PC72.1 - Carlroth) and a dilution with a spore density of 100 spores/ µL (Tween-20 0.1%) was prepared. 10 µL of the spore solution was then applied in the middle of a MEA plate and 3 plates each were incubated at 28°C / 30°C / 32,5°C / 35°C / 37°C for 4 days. The growth was measured in mm diameter.

Genome sequencing and gene prediction

The genome sequencing and assembly of *Cephalotrichum gorgonifer* was performed using a whole-genome shotgun approach that explored paired-end 454 (LGC Genomics GmbH, Berlin, Germany). Using Newbler v2.6. (Roche (2010) 454 Sequencing System Software Manual, v 2.5.3: Part C – GS De Novo Assembler, GS Reference Mapper, SFF Tools, 454. Life Sciences Corp, A Roche Company, Branford) shotgun and 8kb-PE library reads were assembled into 702 contigs. Pre-assembled contigs were combined into 48 scaffolds using the SSPACE algorithm (77). To predict genes on the scaffolds two ab initio gene predictor algorithms were applied, GeneMark-S and GenMark-ES version 2.3 (78). Gene models differently predicted by the algorithms were manually curated. The genome was analysed using the PEDANT system (79) to allow comparative feature analysis.

Transcriptome: RNA sequencing and analysis

Total RNA extraction samples (24h/ 48h; 6 µg each) were transferred to Vienna Biocenter Core Facilities (80) for library preparation and Illumina high throughput sequencing using poly-A enrichment kit (NEB) and Nextera Library prep kit. 50 bp single end sequencing was performed using a HiSeq v4 Illumina sequencer. Obtained sequences were de-multiplexed, quality controlled, filtered using trimmomatic 0.36 (81) and mapped on the *Cephalotrichum gorgonifer* NG_p51 genome assembly (ENA project number PRJEB15373). Mapping was performed using BWA (82). Mapping data were processed using samtools (83) and duplicate reads were removed using Picard MarkDuplicates accessible at (84). Reverse transcripts were counted using python script HTSeq (85). Normalization and statistics were done using R/Bioconductor and the limma and edgeR packages, using mean-variance weighting (voom) and TMM normalisation (86) and robust linear model fitting. A significance cut-off of $p < 0.05$ and an absolute difference of 1 (i.e. 2-fold regulation) was applied for analysis. Transcription levels are log2 read counts per kilobase of exon per million library reads (RPKM). For trace graphs transcript coverage was calculated using bedtools genomecov (87, 88) for each bp normalized to sequencing library sizes as log2 scaled counts per million reads (CPM). All data are available at NCBI GEO under the accession number GSE217303.

Molecular biology methods:

For gDNA extraction, *Cephalotrichum gorgonifer* colonies were inoculated in 1 mL liquid Czapek DOX media with 10 mM NO_3 in Lysing Matrix A tubes (MP Biomedicals; Irvine, CA; Art.No.: SKU 116910100) for 24–48 hours at 30 degrees and 180 rpm. After incubation, the cultures were centrifuged at 20238 rcf in an Eppendorf 5424 centrifuge. The supernatant was removed and 1 mL CENIS lysis buffer (200 mM TRIS-HCl pH 8.5, 250 mM NaCl, 25 mM EDTA, 0.5% SDS) was added. A FastPrep-24™ ribolyzer (MP Biomedicals; Irvine, CA; Art.No.: SKU116004500) was then used to homogenize the samples (20 seconds, 6.0 m/s) and the gDNA extraction according to CENIS was conducted (89). The dried gDNA was dissolved in 100 µL of dH_2O and heated up to 65°C for 10 minutes. 1 µL was taken for PCR.

Polymerase Chain Reaction (PCR) was either performed with the Q5®-polymerase from New England Biolabs (New England Biolabs; Art. No.: M0491L) for plasmid cloning, or with the GoTaq® Green Master Mix (Promega; Madison, WI, USA; Art. No.:M7845) if used for diagnostic PCRs (i.e. strain and plasmid verification). PCR was performed according to the respective manual. Plasmid preparations were performed with Genejet® Plasmid Miniprep Kit (Thermo Scientific™, Art. No.: K0503). All information (primer pair names and sequences, amplicon names and templates) can be retrieved from Additional_file_1.pdf Table S1.

Plasmid construction was performed with either NEBBuilder® HiFi DNA Assembly Master Mix (New England Biolabs (NEB); Art. No.: E2621S) or by yeast recombinational cloning (YRC) (90). All PCR fragments were purified with the Monarch PCR & DNA Cleanup Kit (NEB; Art. No.: T1030L), measured at a NanoDrop™ spectrophotometer (Thermo Fisher Scientific™; Art. No.: ND-2000C). All reactions were conducted according to the manufacturer's manual. All resulting plasmids were verified by sequencing ("Ready2Run" by LGC Genomics GmbH; Berlin, Germany). The plasmids can be retrieved in GenBank format from the additional files (Additional_file_4.gbk to Additional_file_7.gbk). A summary of all plasmids that have been constructed during this study and their main elements is contained in Table 2.

Table 2
Plasmids constructed and used during this study. All plasmids can be retrieved from the additional files in genbank format.

Plasmid	Main Elements	Backbone
pAt-DNG02774	replacement cassette DNG02774 - *A. tumefaciens* transformation backbone	pCBRS
pCas9-DNG02774-sgRNA5	pCas9-hph plus sgRNA for DNG02774	pCas9-hph
pCas9-hph	pCas9-scaff plus hygromycin marker	pCas9-scaff
pCas9-scaff	Cas9–1/2 AMA1 - sgRNA scaffold	-

For construction of the *Agrobacterium tumefaciens* transformation plasmid pAt-DNG02774, plasmid pCBRS (91) and gDNA from *C. gorgonifer* strain NG_p51 were taken as templates for PCR with Q5 polymerase. Q5 products Q5_At_02774_1 to Q5_At_02774_5 (Additional_file_1.pdf Table S1) were used for YRC. The correct assembly was verified by restriction digest of the resulting plasmid with MlsI from Thermo Scientific. The plasmid contains the features needed for agrobacterium mediated transformation and an exchange cassette which replaces the first 2300 base-pairs of gene DNG_02774 (i.e.: CgPKS4) with the hph marker.

For plasmid pCas9-DNG02774-sgRNA5 which was used for the Cas9 mediated mutation of DNG_02774, the two precursor plasmids, pCas9-scaff and pCas9-hph were constructed.

pCas9-scaff was assembled by using HiFi and PCR fragments Q5-Cas9-Scaff-1 to Q5-Cas9-Scaff-7 (Additional_file_1.pdf Table S1). Templates for the PCRs were the plasmid pFC331 (54), gDNA from an *Aspergillus fumigatus* wild-type isolate (in-house strain collection AIT-#1232), gDNA from *Aspergillus nidulans WIM 126* (92), plasmid psgRNA (93), plasmid pCSN44 (94) and the plasmid pRS426 (95).

For the construction of pCas9-hph, plasmid pCas9-scaff was cut with Eco72I (Thermo Scientific™; Art. No.: ER0361) and used for HiFi assembly with PCR fragment Q5-Cas9-hph that contains the hph marker (Additional_file_1.pdf Table S1).

For construction of plasmid pCas9-DNG02774-sgRNA5, plasmid pCas9-hph was cut with Bsp1407I (Thermo Scientific™; Art. No.: ER0932), and assembled together with an sgRNA oligonucleotide with the sequence 5'-gtaccagacgaatctacacaCAAGGACTGATGAGTCCGTGAGGACGAAACGAGTAAGCTCGTCTCCTTGACGAAGTAGCCACCgttttagagctagaaatagc-3'. The sgRNA has the sequence: 5'- TCCTTGACGAAGTAGCCACC | GGG(PAM)-3' and anneals around base pair 275 downstream of the start codon of CgPKS4 (DNG_02774).

Strain construction:

All fungal strains used during this study are listed in Table 3.

Table 3
Fungal strains used during this study. All strains apart from the wildtype NG_p51 have been generated during this study

Strain	Genotype	Parent strain	Transformed vector
C. gorgonifer NG_p51	wildtype strain	-	-
Cg-Cas9-02774-1	ΔDNG_02774	C. gorgonifer NG_p51	pCas9-DNG02774-sgRNA5
Cg-At-02774-1	DNG_02774::hph	C. gorgonifer NG_p51	pAt-DNG02774
Cg-HDR-02774-1	DNG_02774::hph	C. gorgonifer NG_p51	PCR (HDR-Fragment)

Agrobacterium transformation:

Strain Cg-At-02774-1 was generated by disruption of CgPKS4 by agrobacterium mediated transformation with plasmid pAt-DNG02774. The transformation was conducted according to Hanif et al. 2002 (96) and Gorfer et al. 2007 (97) with the deviation that fungal cultures were pre-grown on CM-agar plates and that for co-cultivation of bacteria and fungi, not cellophane or agar-blocks were used, but 200µL of a 1:1 mixture of a fungal spore solution ($1*10^6$ spores/mL in Tween-20 0.1%) and an induced *Agrobacterium* culture broth (*Agrobacterium tumefaciens* carrying pAt-DNG02774) were plated on 10 MoserIND petri dishes each. After 4 days of incubation at 20°C,

the plates were overlain with 15 mL of ~ 40°C warm selection media (YES + hygromycinB + cefotaxim) and incubated for further 3 days at 30°C before picking transformants. After purification *via* single spore isolation, the proper insertion of the replacement cassette was verified by Q5®-PCR with primer pair At-HDR_Diag (Additional_file_1.pdf Table S1) which amplifies the region that spans from outside of the homology regions and across the whole insert. The proper integration was assessed via size comparison of amplicons of the recipient strain (i.e. NG_p51) and the mutant on an agarose gel.

Disruption of CgPKS4 by protoplast transformation (Cas9 and HDR)

For the disruption of gene DNG_02774 by Cas9 (i.e. Cg-Cas9-02774-1) or by a linear fragment (HDR; i.e. Cg-HDR-02774-1), 10 µg plasmid pCas9-DNG02774-sgRNA5 respectively 72 µL of an un-purified Q5®-PCR product (i.e. "HDR-fragment" which is the exact same replacement cassette as within pAt-DNG02774; (Additional_file_1.pdf Table S1) was transformed via a modified protoplast transformation protocol into strain NG_p51 as described below. In case of the Cas9 approach, successful disruption was verified by amplification of the promoter and 5' end of the gene DNG_02774 (~ 2 kb) with primer pair Cas9-Diag (Additional_file_1.pdf Table S1) which showed a 600 base-pair deletion, starting at the sgRNA annealing site. The deletion was further confirmed by sequencing with primer 5'- ATCACTCCCATAGCCGTCATCG3 -3' at the LGC genomics sequencing facility (Berlin, Germany). In case of the HDR approach, the whole replacement cassette was amplified from outside of the homology regions, exactly as described above for the verification of the agrobacterium transformation (i.e. Cg-At-02774-1).

Modified protoplastation and transformation protocol for C. gorgonifer.

For protoplast preparation, spores were harvested with Tween® 20 0.1% from a yeast extract sucrose (YES) agar plate and filtered through a glass wool tip. 6 mL of YES-broth in an eprouvette were inoculated with a spore density of $4*10^6$ spores per mL media and incubated for 18 hours at 30°C at 180 rpm. The culture was transferred into a falcon tube and centrifuged for 5 minutes at 4°C and 2218 rcf in a 5810 R Eppendorf centrifuge with swingout rotor. The supernatant was discarded and 1 mL of Lysing solution was prepared: 12.5 mg Driselase from Basidiomycetes (Sigma- Aldrich; Art. No.: D9515), 1 mg Chitinase, from *Streptomyces griseus* (Sigma- Aldrich; Art. No.: C6137), 25 mg Lysing enzymes from *Trichoderma harzianum* (Sigma- Aldrich; Art. No.: L1412) in 1 mL of "OsmoStock" solution (40 mM/L Citric acid, 1.1 mM/L $MgSO_4$; set pH to 5.9 with 3 mol/L NaOH). The Lysing solution was added to the mycelium. The mixture was resuspended and transferred into 2 mL tubes and put into an "IKA KS4000 I control" shaker at 30°C at 110 rpm for 5 hours. After visual check of protoplasts, the mixture was centrifuged at 4°C for 10 minutes at 6000 rcf in an Eppendorf 5424R centrifuge and as much intermediate layer (clean protoplasts on top, protoplasts and cell debris at bottom) as possible was removed. Protoplasts count was determined in a counting chamber (Neubauer improved; PC72.1 – Carl Roth, Karlsruhe).

For preparation of protoplast kryo-stocks, the solution was set to $4*10^8$ protoplasts per mL with OsmoStock solution and the same amount of 50% glycerol was added and mixed. Aliquots of 90 µL were then slowly frozen in 1.5 mL Eppendorf tubes within two styro-foam boxes at -80°C. Each tube holds protoplasts for 3 transformations (i.e.: $6*10^6$ protoplasts per transformation).

For protoplast transformation, one protoplast kryo-stock was thawed on ice. 6*10^6 protoplasts (i.e. 30 µL) were taken and adjusted to 200 µL with ice-cold TN1 solution (i.e. modified STC buffer solution: Sorbitol 0.8 mol/L, $CaCl_2$ 50 mM/L, Tris-HCl pH 8 10 mM/L) (98). 10 µg plasmid DNA (i.e.: pCas9-DNG02774-sgRNA5) or 72 µL of non-purified Q5-PCR product HDR-fragment (Additional_file_1.pdf Table S1) and 50 µL of ice-cold TN2 (= TN1 with PEG 4000 40% (w/v)) solution were added and mixed gently per pipetting. The whole mixture was left on ice. After 30 minutes, 1 mL of TN2 solution was added, gently mixed and left at room temperature for 5 minutes. The mixture was then added to 45 mL of ~ 40°C Bottom Agarose (AMM (99) + 0.8 mol/L Sucrose + 10mM/L $NaNO_3$ + 0.8% w/v low melt agarose (Carl Roth; Art. No.: 6351.2) and equally distributed into 3 petri dishes. After 2 hours at room temperature, 15 mL of 45°C Top agarose (same recipe as Bottom Agarose but 1.5% (w/v) low melt agarose and 0.05 mg/mL hygromycin B (Merck Millipore; Art. No.: US1400052; potency: 1140 µg/mg) was added to each plate. After solidification, plates were incubated at 30°C until colonies appeared on the surface (~ 7 days). Colonies were picked and two rounds of single spore isolation (strike out – pick – grow until sporulation) were conducted on Aspergillus complete media agar plates (CM by DR. C. F. Robert (99)) with hygromycinB before preparing spore kryo-stocks.

Spore-kryo stock preparation:

The fungus was grown on a CM plate and incubated for 6 days at 30°C. A spore suspension with Tween-20 0.1% (v/v) was prepared, mixed with a 50% (w/v) glycerol solution at a ratio of 1:1 and 5*750 µL aliquots were frozen at -80°C.

Fermentation and extraction for rasfonin standard preparation

Fermentation conditions, isolation and structural elucidation was carried out according to Labuda et al. (100). The fungal spore suspension (5.0 x 10^6 spores/mL) was obtained after 7 days cultivation of the fungus (*Cephalotrichum gorgonifer* NG_p51) on a potato dextrose agar (PDA, VWR Chemicals, Austria). Five colony plugs were cut (each ca 1 x 1 cm) and thoroughly mixed (on vortex for 2 minutes) with 30 mL of physiological solution (0.9% NaCl) in a sterile, 50 mL Falcon tube. In total, 2 kg of parboiled rice was used as a production substrate. Briefly, a total of 100 g of rice mixed with 100 mL deionized water was let soaked for ca one hour in 1000 mL capacity Erlenmeyer flasks, and then sterilized under standard autoclaving conditions (20 min, 121°C, under pressure). Each flask (n = 20) was inoculated with 100 µL of spore suspension at the central part of the surface. The flasks were cultivated in perforated plastic bags for 28 days at 30°C in the dark. At the end of the cultivation, the rice cultures were checked for purity, cut into small pieces and the whole content of the plates (fungal colonies with rice-substrate) was harvested into a 5 L glass flask. No heating deactivation nor drying was performed. The material was then mixed with 2 L of acetonitrile (ACN, Honeywell, Seelze, Germany). After vigorous stirring for 2 min in three subsequent steps (with ca 20 min in between), the mixture was filtered through a steel sieve in order to separate the solid particles (fungus and medium). The remaining residual water (generated by condensation of the water on plates during fungal growth) was removed by the addition of 10 g of anhydrous sodium sulphate. The organic phase was then filtered through a filter paper (270 mm i.d., Macherey-Nagel, Düren, Germany) and concentrated under reduced pressure at 45°C (Büchi Rotavapor R-114, Flawil, Switzerland). The whole extraction procedure was repeated twice and yielded 3.5 g of crude culture extract.

Isolation of secondary metabolites for rasfonin standard preparation

The crude extract was purified by reversed-phase silica gel vacuum flash chromatography (Interchim, puriFlash®450, Montlucon Cedex, France), using three consecutive Interchim puriFlash® 32 g silica IR-50C18-F0025 flash columns (particle size: 50µm). The columns were eluted with a binary solvent gradient (solvent A: H_2O, solvent B: ACN). The starting linear gradient from 10% B to 27% B during 25 min at a flow rate 15 mL/min was followed by an isocratic gradient at 52% B for 10 min. Then a linear gradient from 52–66% B over 7min was applied at the same flow rate and finally the column was washed starting with 100% B for 10 min followed by 100% A for 10 min at a flow rate 15–30 mL/min. UV 254 nm and UV scan 200–400 nm mode were used for detection and final separation of 7 main fractions (F1-F7), which were consequently concentrated under reduced pressure at 45°C. The target compound was found in fraction F5 (23–27 R_t, yield: 370 mg). It was resolved in a solvent mix (1:1:1; ACN/CH_3OH/H_2O) and further purified by an Agilent 1260 Infinity preparative HPLC (USA) on a reversed phase column Gemini NX C-18 (21.20 x 150 mm, 5 µm, 110 Å). Gradient starting with 30% ACN and 70% H_2O up to 90% ACN in 10min (total time 34 min) and a flow rate of 25 ml/min. Four fractions (pF1 -pF4, time slice each 0.5 min) were collected, of which pF4 contained the target- rasfonin. Yield of rasfonin in pF4 (t_R 17.85–18.70 min) after one stage of prep HPLC was 250 mg. For purity check an Agilent 1200 system was used with the same stationary phase and gradient program (Gemini 5 µm NX-C18 110 Å, 150 x 2 mm) and gradient program at a flow rate 0.3 mL/min. Analytical chromatogram of purified rasfonin and its UV spectrum is presented on Figure S 3 in Additional_file_1.pdf. The identity of rasfonin was furthermore verified by NMR analysis (see below).

LC-HRMS

LC-HRMS measurements were carried out with a Vanquish UHPLC system coupled to a QExactive HF Orbitrap mass spectrometer (Thermo Fisher Scientific). For chromatographic separation a C18 reversed phase column (X-Bridge, 150x2.1mm id, 3.5µm particle size, Waters) was used with gradient elution applying H2O + 0.1% FA (eluent A) and methanol + 0.1% FA (eluents B) as eluents with a constant flow rate of 0.25 ml/min. After an initial minute with constant 10% eluent B, a linear increase towards 100% B was applied in 9 minutes followed by 3 constant minutes of 100% B. 7 minutes of re-equilibration with 10% B completed the method with a total length of 20 minutes. Ionisation was carried out in fast polarity switching mode and full scan mass spectra were recorded with a mass range of m/z 100–1000 and a resolution of 120 000 at *m/z* 200 (FWHM). MS/MS measurements for $[M + H]^+$ of Rasfonin were carried out in a data dependant method using an inclusion list. The selected ions were fragmented with stepped normalized collision energy (25, 35, 45 eV) and recorded with a resolution of 15 000 at *m/z* 200 (FWHM) at mass ranges *m/z* 50 to 460. For compound identification the in-house purified reference standard of Rasfonin (see above) was dissolved and diluted to a concentration of 1 mg/L and measured with the described method within the same sequence as all biological samples.

NMR

All NMR spectra were recorded on a Bruker Avance II 400 (resonance frequencies 400.13 MHz for ^1H and 100.63 MHz for ^{13}C) equipped with a 5 mm N_2-cooled cryoprobe (Prodigy) with z–gradients at room temperature with standard Bruker pulse programs. The sample was dissolved in 0.6 mL of $CDCl_3$ (99.8% D). Chemical shifts are given in ppm, referenced to residual solvent signals (7.26 ppm for ^1H, 77.0 ppm for ^{13}C). ^1H NMR data were collected with 32k complex data points and apodised with a Gaussian window function (lb = – 0.3 Hz

and gb = 0.3 Hz) prior to Fourier transformation. ^{13}C spectrum with WALTZ16 ^{1}H decoupling was acquired using 64k data points. Signal-to-noise enhancement was achieved by multiplication of the FID with an exponential window function (lb = 1Hz). All two-dimensional experiments were performed with 1k × 256 data points, while the number of transients (2–16 scans) and the sweep widths were optimized individually. HSQC experiment was acquired using adiabatic pulse for inversion of ^{13}C and GARP-sequence for broadband ^{13}C-decoupling, optimized for $^{1}J(CH)$ = 145 Hz. For the NOESY spectrum a mixing time of 0.5 s was used.

Structure determination of rasfonin (Fig. 4) standard by NMR

Table 4

^{1}H and ^{13}C nmr data of rasfonin in CDCl3

	^{1}H	^{13}C
1	-	163.29
2	6.21, d, 1H, *J* = 9.6	124.93
3	7.04, dd, 1H, *J* = 9.6; 6.0	140.58
4	5.34, dd, 1H, *J* = 6.0; 2.5	61.70
5	4.13, dd, 1H, *J* = 8.9; 2.5	83.28
6	2.18, m, 1H	31.37
7	1.21, ddd, 1H, *J* = 13.4; 9.0; 3.9	39.94
	1.03, ddd, 1H, *J* = 13.4; 10.0; 4.8	
8	1.68, m, 1H	27.85
9	2.06, br.d, 1H, *J* = 13.2	46.28
	1.44, dd, 1H, *J* = 13.2; 9.8	
10	-	134.18
11	5.12, br.q, 1H, *J* = 7.1	120.04
12	1.54, br.d, 3H, *J* = 7.1	13.33
13	1.15, d, 3H, *J* = 6.6	18.85
14	0.78, d, 3H, *J* = 6.5	20.59
15	1.52, br.s, 3H	15.53
1’	-	168.08
2’	5.81, d, 1H, *J* = 15.6	115.01
3’	7.34, dd, 1H, *J* = 15.6; 0.5	150.96
4’	-	134.63
5’	5.77, br.d, 1H, *J* = 9.9	143.28
6’	2.88, m, 1H	39.22
7’	1.79 + 1.61, each m, 1H	34.74
8’	3.73, dt, 1H, *J* = 10.6; 5.5	60.60
	3.60, m, 1H	
9’	1.83, d, 3H, *J* = 1.2	12.59
10’	3.60, m, 2H	65.81

The isolated compound showed a $[M + H]^{+}$ peak at *m/z* = 435.2697 1229 (calcd 435.2741 for $C_{25}H_{39}O_{6}$) in the ESI spectrum which is in accordance with the expected molecular formula of $C_{25}H_{38}O_{6}$. The ^{1}H and ^{13}C nmr spectra revealed the presence of three doubletic

methyl groups at δ_H/δ_C 1.54/13.33, 1.15/18.85, 0.78/20.59 ppm and two singlet methyl groups at 1.52/15.53, and 1.83/12.59 ppm, respectively. In addition, 6 olefinic protons could be detected. Two pairs of them are part from delocalized double bond systems due to conjugation to carboxylic carbons C-1 and C-1': H-2/C-2 and H-3/C-3 showed signals at δ_H/δ_C 6.21/124.93 and 7.04/140.58 ppm, whereas the system 2' and 3' resonated at δ_H/δ_C 5.81/115.01 and 7.34/150.96 ppm, respectively. Furthermore, two oxygenated methines and two oxygenated methylene groups were identified in the nmr spectra. Detailed analysis of all two-dimensional nmr spectra proved the presence of rasfonin for the isolated compound. All assigned chemical shifts (Table 4) are in agreement with those already reported for rasfonin by Fujimoto et al. (101).

Rasfonin analysis of CgPKS4 knock-out strains:

For rasfonin analysis of *CgPKS4*- mutants, triplicates of each knockout strain and the wildtype NG_p51 were cultivated. Fungal spores were plated on YES- agar plates supplemented with 100 mM NO_3 and cultivated at 30°C for 7 days. The culture + agar was then cut into ~ 1 cm^2 pieces, frozen in liquid nitrogen and lyophilised in a Christ Alpha 2–4 LSCbasic lyophilizer. The freeze-dried material was ground in a Retsch MIXER MILL MM 400 ball mill in a liquid nitrogen cooled 50 mL grinding jar with one 20 mm stainless steel grinding ball per jar at 25hz for 60 seconds. 0.1g of the ground material were extracted with 1.5 mL ACN with 0.1% FA acid on an IKA Vibrax VXR basic shaker at 1500rpm for 1 hour at room temperature. The slurry was then centrifuged for 20 minutes at 20238 rcf and at room temperature in an Eppendorf 5424 centrifuge. The supernatant was then filtrated through a 0.22 µM PTFE syringe filter, and the extract was reduced in a prewarmed (45°C) Eppendorf concentrator plus for 30 minutes at V-HV settings. The reduced extracts were refilled to 300 µL with ACN and filtered again to remove precipitate that formed during concentration. The extracts were directly measured in via HPLC and LC-HRMS.

Measurement of knockout-mutants via HPLC:

Samples were analyzed with an Agilent 1200 system with a reversed phase column Phenomenex Gemini NX C-18 (2 x 150 mm, 5 µm, 110 Å). Injection volume of samples was 20 µL. The flow rate was 0.3 mL/min with a binary gradient of A from 15% (ACN + 0.1% FA) to 95% in the time interval 2 minutes to 31 minutes (Solvent B: MQ-H_2O + 0.1% FA). Rasfonin was detected with an Agilent G1315C DAD detector at 280nm. Elution time of rasfonin was at around 21.1 minutes. For reference measurement and sample spiking, a 25 µg/mL rasfonin standard produced by our laboratory (see above) was used.

Declarations

Ethics approval and consent to participate: Not applicable

Consent for publication: Not applicable

Availability of data and materials:

The datasets that were generated during this study are accessible at following repositories:

Genome and Gene annotation of *C. gorgonifer* NG_p51: European Nucleotide Archive (ENA) at EMBL-EBI. Project number PRJEB15373 which can be accessed at http://www.ebi.ac.uk/ena/data/view/ONZQ01000001-ONZQ01000048 (40)

Transcriptome data of *C. gorgonifer* NG_p51 at 24h and 48h: The data discussed in this publication have been deposited in NCBI's Gene Expression Omnibus (46) and are accessible through GEO Series accession number GSE217303 (https://www.ncbi.nlm.nih.gov/geo/query/acc.cgi?acc=GSE217303).

The datasets supporting the conclusions of this article are included within the article and its additional files.

Competing interests: The authors declare that they have no competing interests.

Funding: Open access funding provided by Austrian Science Fund (FWF). Work was funded by grant LS19-009 "TASSMATA" and "Bioactive Microbial Metabolites" grant K3-G-2/08-2020 from the NFB Lower Austria Science Fund and grant P32790 "ChroCosm" from the FWF Austrian Science Fund to Joseph Strauss.

Authors' contributions

AS (study design, protocol establishment, micro- and molecular biology, figures, writing), LSR (Biosynthesis pathway of rasfonin, linking of rasfonin to BGC, study design, writing, figures), HB (Transcriptome analysis, BGC prediction), LS (chemical analysis, preliminary data

acquisition), RL (Species description, morphology, rasfonin standard preparation and verification, figures), UG (Genome assembly, Gene annotation), MG (Agrobacterium Trafo, Isolation, strain information and identification), MB (NMR analysis), MD (LC-HRMS chemical analysis), EG (HPLC rasfonin method establishment and detection), AG (HPLC-chemical analysis), MS (screening, chemical analysis), JS (Funding acquisition, study design, manuscript writing)

Acknowledgements: We want to thank colleagues from the Mortensen laboratory (Technical University of Denmark, Søltofts Plads, Kongens Lyngby, Denmark) that provided the plasmid templates (pFC331) for the Cas9 gene and the AMA1 region. We are also thankful to Dragana Bandian (AIT, Austrian Institute of Technology) who provided the gDNAs of fungal wild-type isolates for plasmid construction.

References

1. Liu Y-N, Zhang T-J, Lu X-X, Ma B-L, Ren A, Shi L, et al. Membrane fluidity is involved in the regulation of heat stress induced secondary metabolism in Ganoderma lucidum. Environmental Microbiology. 2017;19(4):1653-68.
2. Overy D, Correa H, Roullier C, Chi WC, Pang KL, Rateb M, et al. Does Osmotic Stress Affect Natural Product Expression in Fungi? Mar Drugs. 2017;15(8).
3. Wong HJ, Mohamad-Fauzi N, Rizman-Idid M, Convey P, Alias SA. Protective mechanisms and responses of micro-fungi towards ultraviolet-induced cellular damage. Polar Science. 2019;20:19-34.
4. Scherlach K, Sarkar A, Schroeckh V, Dahse H-M, Roth M, Brakhage AA, et al. Two Induced Fungal Polyketide Pathways Converge into Antiproliferative Spiroanthrones. ChemBioChem. 2011;12(12):1836-9.
5. Zehetbauer F, Seidl A, Berger H, Sulyok M, Kastner F, Strauss J. RimO (SrrB) is required for carbon starvation signaling and production of secondary metabolites in Aspergillus nidulans. Fungal Genetics and Biology. 2022;162:103726.
6. Wang G, Ran H, Fan J, Keller NP, Liu Z, Wu F, et al. Fungal-fungal cocultivation leads to widespread secondary metabolite alteration requiring the partial loss-of-function VeA1 protein. Science Advances. 2022;8(17):eabo6094.
7. Bazafkan H, Dattenböck C, Böhmdorfer S, Tisch D, Stappler E, Schmoll M. Mating type-dependent partner sensing as mediated by VEL1 in Trichoderma reesei. Molecular Microbiology. 2015;96(6):1103-18.
8. Pusztahelyi T, Holb I, Pócsi I. Secondary metabolites in fungus-plant interactions. Frontiers in Plant Science. 2015;6.
9. Alarcón J, Águila S. Lovastatin Production by Pleurotus ostreatus: Effects of the C:N Ratio. Zeitschrift für Naturforschung C. 2006;61(1-2):95-8.
10. Ziemons S, Koutsantas K, Becker K, Dahlmann T, Kück U. Penicillin production in industrial strain Penicillium chrysogenum P2niaD18 is not dependent on the copy number of biosynthesis genes. BMC Biotechnology. 2017;17(1):16.
11. Atongbiik Achaglinkame M, Opoku N, Amagloh FK. Aflatoxin contamination in cereals and legumes to reconsider usage as complementary food ingredients for Ghanaian infants: A review. Journal of Nutrition & Intermediary Metabolism. 2017;10:1-7.
12. Farhadi A, Fakhri Y, Kachuei R, Vasseghian Y, Huseyn E, Mousavi Khaneghah A. Prevalence and concentration of fumonisins in cereal-based foods: a global systematic review and meta-analysis study. Environ Sci Pollut Res Int. 2021;28(17):20998-1008.
13. Giorni P, Bertuzzi T, Battilani P. Impact of Fungi Co-occurrence on Mycotoxin Contamination in Maize During the Growing Season. Frontiers in Microbiology. 2019;10.
14. Keller NP. Fungal secondary metabolism: regulation, function and drug discovery. Nat Rev Microbiol. 2019;17(3):167-80.
15. Sørensen T, Petersen C, Fechete LI, Nielsen KL, Sondergaard TE. A Highly Contiguous Genome Assembly of Arthrinium puccinoides. Genome Biology and Evolution. 2022;14(1):evac010.
16. Graham-Taylor C, Kamphuis LG, Derbyshire MC. A detailed in silico analysis of secondary metabolite biosynthesis clusters in the genome of the broad host range plant pathogenic fungus Sclerotinia sclerotiorum. BMC Genomics. 2020;21(1):7.
17. Blackwell M. The fungi: 1, 2, 3 ... 5.1 million species? Am J Bot. 2011;98(3):426-38.
18. Gorfer M, Blumhoff M, Klaubauf S, Urban A, Inselsbacher E, Bandian D, et al. Community profiling and gene expression of fungal assimilatory nitrate reductases in agricultural soil. The ISME Journal. 2011;5(11):1771-83.
19. Klaubauf S, Inselsbacher E, Zechmeister-Boltenstern S, Wanek W, Gottsberger R, Strauss J, et al. Molecular diversity of fungal communities in agricultural soils from Lower Austria. Fungal Diversity. 2010;44(1):65-75.
20. Gorfer M, Klaubauf S, Berger H, Strauss J. The fungal contribution to the nitrogen cycle in agricultural soils. 2014. p. 209-25.
21. Collemare J, Seidl MF. Chromatin-dependent regulation of secondary metabolite biosynthesis in fungi: is the picture complete? FEMS Microbiology Reviews. 2019;43(6):591-607.

22. Gacek A, Strauss J. The chromatin code of fungal secondary metabolite gene clusters. Applied Microbiology and Biotechnology. 2012;95(6):1389-404.
23. Pfannenstiel B, Keller N. On top of biosynthetic gene clusters: How epigenetic machinery influences secondary metabolism in fungi. Biotechnology Advances. 2019;37.
24. Reyes-Dominguez Y, Bok JW, Berger H, Shwab EK, Basheer A, Gallmetzer A, et al. Heterochromatic marks are associated with the repression of secondary metabolism clusters in Aspergillus nidulans. Molecular microbiology. 2010;76(6):1376-86.
25. Schüller A, Studt-Reinhold L, Strauss J. How to Completely Squeeze a Fungus—Advanced Genome Mining Tools for Novel Bioactive Substances. Pharmaceutics. 2022;14(9):1837.
26. Zutz C, Bacher M, Parich A, Kluger B, Gacek-Matthews A, Schuhmacher R, et al. Valproic Acid Induces Antimicrobial Compound Production in Doratomyces microspores. Frontiers in Microbiology. 2016;7.
27. Bachleitner S, Sørensen JL, Gacek-Matthews A, Sulyok M, Studt L, Strauss J. Evidence of a Demethylase-Independent Role for the H3K4-Specific Histone Demethylases in Aspergillus nidulans and Fusarium graminearum Secondary Metabolism. Front Microbiol. 2019;10:1759.
28. Gacek-Matthews A, Berger H, Sasaki T, Wittstein K, Gruber C, Lewis ZA, et al. KdmB, a Jumonji Histone H3 Demethylase, Regulates Genome-Wide H3K4 Trimethylation and Is Required for Normal Induction of Secondary Metabolism in Aspergillus nidulans. PLOS Genetics. 2016;12(8):e1006222.
29. Niehaus E-M, Rindermann L, Janevska S, Münsterkötter M, Güldener U, Tudzynski B. Analysis of the global regulator Lae1 uncovers a connection between Lae1 and the histone acetyltransferase HAT1 in Fusarium fujikuroi. Applied Microbiology and Biotechnology. 2018;102(1):279-95.
30. Atanasoff-Kardjalieff AK, Studt L. Secondary Metabolite Gene Regulation in Mycotoxigenic Fusarium Species: A Focus on Chromatin. Toxins (Basel). 2022;14(2).
31. Sulyok M, Stadler D, Steiner D, Krska R. Validation of an LC-MS/MS-based dilute-and-shoot approach for the quantification of > 500 mycotoxins and other secondary metabolites in food crops: challenges and solutions. Anal Bioanal Chem. 2020;412(11):2607-20.
32. Hou B, Liu S, Li E, Jiang X. Different Role of Raptor and Rictor in Regulating Rasfonin-Induced Autophagy and Apoptosis in Renal Carcinoma Cells. Chemistry & Biodiversity. 2020;17(12):e2000743.
33. Lu Q, Yan S, Sun H, Wang W, Li Y, Yang X, et al. Akt inhibition attenuates rasfonin-induced autophagy and apoptosis through the glycolytic pathway in renal cancer cells. Cell Death Dis. 2015;6(12):e2005.
34. Xiao Z, Li L, Li Y, Zhou W, Cheng J, Liu F, et al. Rasfonin, a novel 2-pyrone derivative, induces ras-mutated Panc-1 pancreatic tumor cell death in nude mice. Cell Death & Disease. 2014;5(5):e1241-e.
35. Zhang F, Yan TQ, Guo W. [Rasfonin inhibits proliferation and migration of osteosarcoma 143B cells]. Beijing Da Xue Xue Bao Yi Xue Ban. 2019;51(2):234-8.
36. Sandoval-Denis M, Guarro J, Cano-Lira JF, Sutton DA, Wiederhold NP, de Hoog GS, et al. Phylogeny and taxonomic revision of Microascaceae with emphasis on synnematous fungi. Studies in Mycology. 2016;83(1):193-233.
37. Woudenberg JHC, Sandoval-Denis M, Houbraken J, Seifert KA, Samson RA. Cephalotrichum and related synnematous fungi with notes on species from the built environment. Studies in Mycology. 2017;88(1):137-59.
38. Domsch KH, Gams W, Anderson TH. Compendium of soil fungi. Volume 1. London: Academic Press (London) Ltd.; 1980. viii + 860pp. p.
39. Ellis MB. Dematiaceous Hyphomycetes: Kew, Commonwealth Mycological Institute.; 1971. 608 pp. p.
40. Genome sequence data and gene annotation of Cephalotrichum gorgonifer NG_p51: European Nucleotide Archive; 2022 [Available from: http://www.ebi.ac.uk/ena/data/view/ONZQ01000001-ONZQ01000048.
41. Westphal KR, Muurmann AT, Paulsen IE, Nørgaard KTH, Overgaard ML, Dall SM, et al. Who Needs Neighbors? PKS8 Is a Stand-Alone Gene in Fusarium graminearum Responsible for Production of Gibepyrones and Prolipyrone B. Molecules. 2018;23(9).
42. Brown DW, Yu JH, Kelkar HS, Fernandes M, Nesbitt TC, Keller NP, et al. Twenty-five coregulated transcripts define a sterigmatocystin gene cluster in Aspergillus nidulans. Proc Natl Acad Sci U S A. 1996;93(4):1418-22.
43. Medema MH, Kottmann R, Yilmaz P, Cummings M, Biggins JB, Blin K, et al. Minimum Information about a Biosynthetic Gene cluster. Nat Chem Biol. 2015;11(9):625-31.
44. Robey MT, Caesar LK, Drott MT, Keller NP, Kelleher NL. An interpreted atlas of biosynthetic gene clusters from 1,000 fungal genomes. Proceedings of the National Academy of Sciences. 2021;118(19):e2020230118.

45. Blin K, Shaw S, Kloosterman AM, Charlop-Powers Z, van Wezel GP, Medema Marnix H, et al. antiSMASH 6.0: improving cluster detection and comparison capabilities. Nucleic Acids Research. 2021;49(W1):W29-W35.
46. Edgar R, Domrachev M, Lash AE. Gene Expression Omnibus: NCBI gene expression and hybridization array data repository. Nucleic Acids Res. 2002;30(1):207-10.
47. Zhou ZZ, Zhu HJ, Lin LP, Zhang X, Ge HM, Jiao RH, et al. Dalmanol biosyntheses require coupling of two separate polyketide gene clusters. Chem Sci. 2019;10(1):73-82.
48. Ugai T, Minami A, Fujii R, Tanaka M, Oguri H, Gomi K, et al. Heterologous expression of highly reducing polyketide synthase involved in betaenone biosynthesis. Chem Commun (Camb). 2015;51(10):1878-81.
49. Bonsch B, Belt V, Bartel C, Duensing N, Koziol M, Lazarus CM, et al. Identification of genes encoding squalestatin S1 biosynthesis and in vitro production of new squalestatin analogues. Chemical Communications. 2016;52(41):6777-80.
50. Trenti F, Cox RJ. Structural Revision and Biosynthesis of the Fungal Phytotoxins Phyllostictines A and B. J Nat Prod. 2017;80(5):1235-40.
51. Chen LH, Lin CH, Chung KR. A nonribosomal peptide synthetase mediates siderophore production and virulence in the citrus fungal pathogen Alternaria alternata. Mol Plant Pathol. 2013;14(5):497-505.
52. Qiao K, Chooi Y-H, Tang Y. Identification and engineering of the cytochalasin gene cluster from Aspergillus clavatus NRRL 1. Metab Eng. 2011;13(6):723-32.
53. Li D, Tang Y, Lin J, Cai W. Methods for genetic transformation of filamentous fungi. Microbial Cell Factories. 2017;16(1):168.
54. Nødvig CS, Nielsen JB, Kogle ME, Mortensen UH. A CRISPR-Cas9 System for Genetic Engineering of Filamentous Fungi. PLoS One. 2015;10(7):e0133085.
55. Jiang Y, Wang D, Yao Y, Eubel H, Künzler P, Møller IM, et al. MULocDeep: A deep-learning framework for protein subcellular and suborganellar localization prediction with residue-level interpretation. Comput Struct Biotechnol J. 2021;19:4825-39.
56. Boenisch MJ, Broz KL, Purvine SO, Chrisler WB, Nicora CD, Connolly LR, et al. Structural reorganization of the fungal endoplasmic reticulum upon induction of mycotoxin biosynthesis. Sci Rep. 2017;7:44296.
57. Menke J, Weber J, Broz K, Kistler HC. Cellular development associated with induced mycotoxin synthesis in the filamentous fungus Fusarium graminearum. PLoS One. 2013;8(5):e63077.
58. Gaffoor I, Trail F. Characterization of Two Polyketide Synthase Genes Involved in Zearalenone Biosynthesis in Gibberella zeae. Applied and Environmental Microbiology. 2006;72(3):1793-9.
59. Lonjon F, Rengel D, Roux F, Henry C, Turner M, Le Ru A, et al. HpaP Sequesters HrpJ, an Essential Component of Ralstonia solanacearum Virulence That Triggers Necrosis in Arabidopsis. Molecular Plant-Microbe Interactions®. 2019;33(2):200-11.
60. Chiang Y-M, Szewczyk E, Davidson AD, Keller N, Oakley BR, Wang CCC. A Gene Cluster Containing Two Fungal Polyketide Synthases Encodes the Biosynthetic Pathway for a Polyketide, Asperfuranone, in Aspergillus nidulans. Journal of the American Chemical Society. 2009;131(8):2965-70.
61. Dalmais B, Schumacher J, Moraga J, Le PÊCheur P, Tudzynski B, Collado IG, et al. The Botrytis cinerea phytotoxin botcinic acid requires two polyketide synthases for production and has a redundant role in virulence with botrydial. Molecular Plant Pathology. 2011;12(6):564-79.
62. Sutherland A, Auclair K, Vederas JC. Recent advances in the biosynthetic studies of lovastatin. Curr Opin Drug Discov Devel. 2001;4(2):229-36.
63. Abe Y, Suzuki T, Ono C, Iwamoto K, Hosobuchi M, Yoshikawa H. Molecular cloning and characterization of an ML-236B (compactin) biosynthetic gene cluster in Penicillium citrinum. Molecular Genetics and Genomics. 2002;267(5):636-46.
64. Wang WG, Wang H, Du LQ, Li M, Chen L, Yu J, et al. Molecular Basis for the Biosynthesis of an Unusual Chain-Fused Polyketide, Gregatin A. J Am Chem Soc. 2020;142(18):8464-72.
65. Atanasoff-Kardjalieff AK, Seidl B, Steinert K, Daniliuc CG, Schuhmacher R, Humpf HU, et al. Biosynthesis of the Isocoumarin Derivatives Fusamarins is Mediated by the PKS8 Gene Cluster in Fusarium. Chembiochem. 2022:e202200342.
66. von Bargen KW, Niehaus EM, Krug I, Bergander K, Würthwein EU, Tudzynski B, et al. Isolation and Structure Elucidation of Fujikurins A-D: Products of the PKS19 Gene Cluster in Fusarium fujikuroi. J Nat Prod. 2015;78(8):1809-15.
67. Wiemann P, Sieber CMK, von Bargen KW, Studt L, Niehaus E-M, Espino JJ, et al. Deciphering the Cryptic Genome: Genome-wide Analyses of the Rice Pathogen Fusarium fujikuroi Reveal Complex Regulation of Secondary Metabolism and Novel Metabolites. PLOS Pathogens. 2013;9(6):e1003475.

68. Xu W, Chooi Y-H, Choi JW, Li S, Vederas JC, Da Silva NA, et al. LovG: The Thioesterase Required for Dihydromonacolin L Release and Lovastatin Nonaketide Synthase Turnover in Lovastatin Biosynthesis. Angewandte Chemie International Edition. 2013;52(25):6472-5.
69. Droce A, Saei W, Jørgensen SH, Wimmer R, Giese H, Wollenberg RD, et al. Functional Analysis of the Fusarielin Biosynthetic Gene Cluster. Molecules [Internet]. 2016; 21(12).
70. Newman AG, Vagstad AL, Belecki K, Scheerer JR, Townsend CA. Analysis of the cercosporin polyketide synthase CTB1 reveals a new fungal thioesterase function. Chemical Communications. 2012;48(96):11772-4.
71. Campbell CD, Vederas JC. Biosynthesis of lovastatin and related metabolites formed by fungal iterative PKS enzymes. Biopolymers. 2010;93(9):755-63.
72. Wu J-D, Chou J-C. Optimization of Protoplast Preparation and Regeneration of a Medicinal Fungus Antrodia cinnamomea. Mycobiology. 2019;47(4):483-93.
73. Kumar S, Stecher G, Li M, Knyaz C, Tamura K. MEGA X: Molecular Evolutionary Genetics Analysis across Computing Platforms. Mol Biol Evol. 2018;35(6):1547-9.
74. Thompson JD, Higgins DG, Gibson TJ. CLUSTAL W: improving the sensitivity of progressive multiple sequence alignment through sequence weighting, position-specific gap penalties and weight matrix choice. Nucleic Acids Res. 1994;22(22):4673-80.
75. Tamura K, Nei M. Estimation of the number of nucleotide substitutions in the control region of mitochondrial DNA in humans and chimpanzees. Mol Biol Evol. 1993;10(3):512-26.
76. Samson RAHJTUFJCAB. Food and indoor fungi2019.
77. Boetzer M, Henkel CV, Jansen HJ, Butler D, Pirovano W. Scaffolding pre-assembled contigs using SSPACE. Bioinformatics. 2010;27(4):578-9.
78. Ter-Hovhannisyan V, Lomsadze A, Chernoff YO, Borodovsky M. Gene prediction in novel fungal genomes using an ab initio algorithm with unsupervised training. Genome Research. 2008;18(12):1979-90.
79. Walter MC, Rattei T, Arnold R, Güldener U, Münsterkötter M, Nenova K, et al. PEDANT covers all complete RefSeq genomes. Nucleic Acids Research. 2009;37(suppl_1):D408-D11.
80. [Vienna Biocenter Core Facilities]. Available from: https://www.viennabiocenter.org/vbcf/.
81. Bolger AM, Lohse M, Usadel B. Trimmomatic: a flexible trimmer for Illumina sequence data. Bioinformatics. 2014;30(15):2114-20.
82. Li H, Durbin R. Fast and accurate short read alignment with Burrows–Wheeler transform. Bioinformatics. 2009;25(14):1754-60.
83. Danecek P, Bonfield JK, Liddle J, Marshall J, Ohan V, Pollard MO, et al. Twelve years of SAMtools and BCFtools. Gigascience. 2021;10(2).
84. [Picard MarkDuplicates]. Available from: https://broadinstitute.github.io/picard/.
85. Anders S, Pyl PT, Huber W. HTSeq—a Python framework to work with high-throughput sequencing data. Bioinformatics. 2015;31(2):166-9.
86. Law CW, Chen Y, Shi W, Smyth GK. voom: precision weights unlock linear model analysis tools for RNA-seq read counts. Genome Biology. 2014;15(2):R29.
87. Quinlan AR, Hall IM. BEDTools: a flexible suite of utilities for comparing genomic features. Bioinformatics. 2010;26(6):841-2.
88. [bedtools genomecov]. Available from: https://bedtools.readthedocs.io/en/latest/content/tools/genomecov.html.
89. Cenis JL. Rapid extraction of fungal DNA for PCR amplification. Nucleic Acids Research. 1992;20(9):2380-.
90. Schumacher J. Tools for Botrytis cinerea: New expression vectors make the gray mold fungus more accessible to cell biology approaches. Fungal Genetics and Biology. 2012;49(6):483-97.
91. Németh MZ, Li G, Seress D, Pintye A, Molnár O, Kovács GM, et al. What is the role of the nitrate reductase (euknr) gene in fungi that live in nitrate-free environments? A targeted gene knock-out study in Ampelomyces mycoparasites. Fungal Biol. 2021;125(11):905-13.
92. Mooney JL, Yager LN. Light is required for conidiation in Aspergillus nidulans. Genes & Development. 1990;4(9):1473-82.
93. Schüller A, Wolansky L, Berger H, Studt L, Gacek-Matthews A, Sulyok M, et al. A novel fungal gene regulation system based on inducible VPR-dCas9 and nucleosome map-guided sgRNA positioning. Applied Microbiology and Biotechnology. 2020;104(22):9801-22.
94. Staben C, Jensen B, Singer M, Pollock J, Schechtman M, Kinsey J, et al. Use of a bacterial hygromycin B resistance gene as a dominant selectable marker in Neurospora crassa transformation. Fungal Genetics Reports. 1989;36(1).

95. Christianson TW, Sikorski RS, Dante M, Shero JH, Hieter P. Multifunctional yeast high-copy-number shuttle vectors. Gene. 1992;110(1):119-22.
96. Hanif M, Pardo AG, Gorfer M, Raudaskoski M. T-DNA transfer and integration in the ectomycorrhizal fungus Suillus bovinus using hygromycin B as a selectable marker. Curr Genet. 2002;41(3):183-8.
97. Gorfer M, Klaubauf S, Bandian D, Strauss J. Cadophora finlandia and Phialocephala fortinii: Agrobacterium-mediated transformation and functional GFP expression. Mycological Research. 2007;111(7):850-5.
98. He Z-M, Price MS, Obrian GR, Georgianna DR, Payne GA. Improved protocols for functional analysis in the pathogenic fungus Aspergillus flavus. BMC Microbiology. 2007;7(1):104.
99. Barratt RW, Johnson GB, Ogata WN. Wild-type and mutant stocks of Aspergillus nidulans. Genetics. 1965;52(1):233-46.
100. Labuda R, Bacher M, Gratzl H, Doppler M, Parich A, Aufy M, et al. Luteapyrone, a Novel -Pyrone Isolated from the Filamentous Fungus Metapochonia lutea. Molecules. 2021;26(21):6589.
101. Fujimoto H, Okamoto Y, Sone E, Maeda S, Akiyama K, Ishibashi M. Eleven New 2-Pyrones from a Fungi Imperfecti, Trichurus terrophilus, Found in a Screening Study Guided by Immunomodulatory Activity. Chemical and Pharmaceutical Bulletin. 2005;53(8):923-9.

Figures

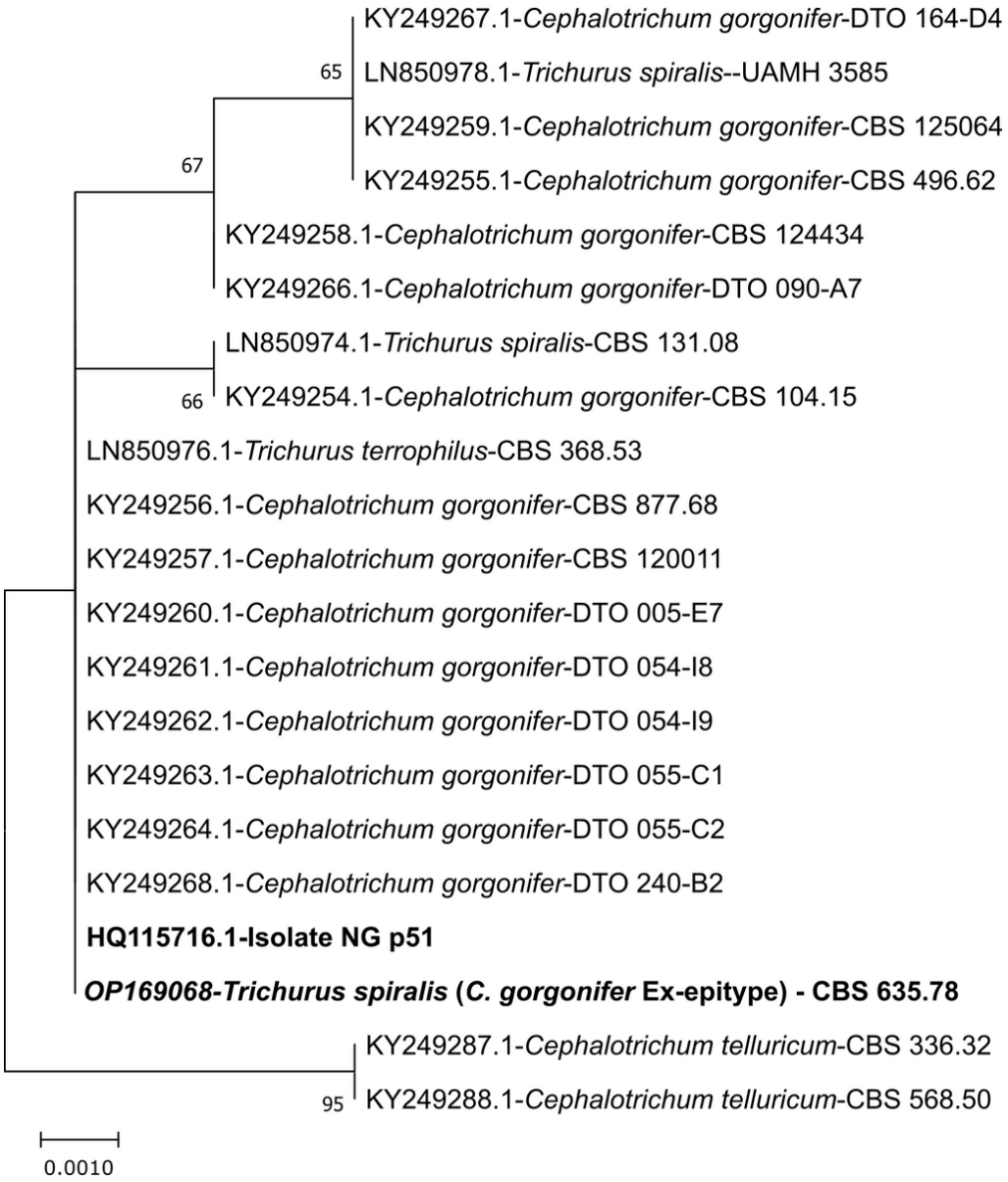

Figure 1

Phylogenetic tree of Cehpalotrichum gorgonifer isolate NG_p51

A: Phylogenetic tree based on the ITS sequences of strain isolate NG_p51 together with several Cephalotrichum gorgonifer isolates and C. telluricum strains as closest. The tree entries follow following pattern: “accession number- genus and species-isolate identifier”. The phylogenetic analysis shows that strain isolate NG_p51 belongs to the species Cephalotrichum gorgonifer. The tree is drawn to scale, with branch lengths measured in the number of substitutions per site. The strain isolate (i.e. NG_p51) used for all experiments in this publication and the Ex-epitype are written in bold letters.

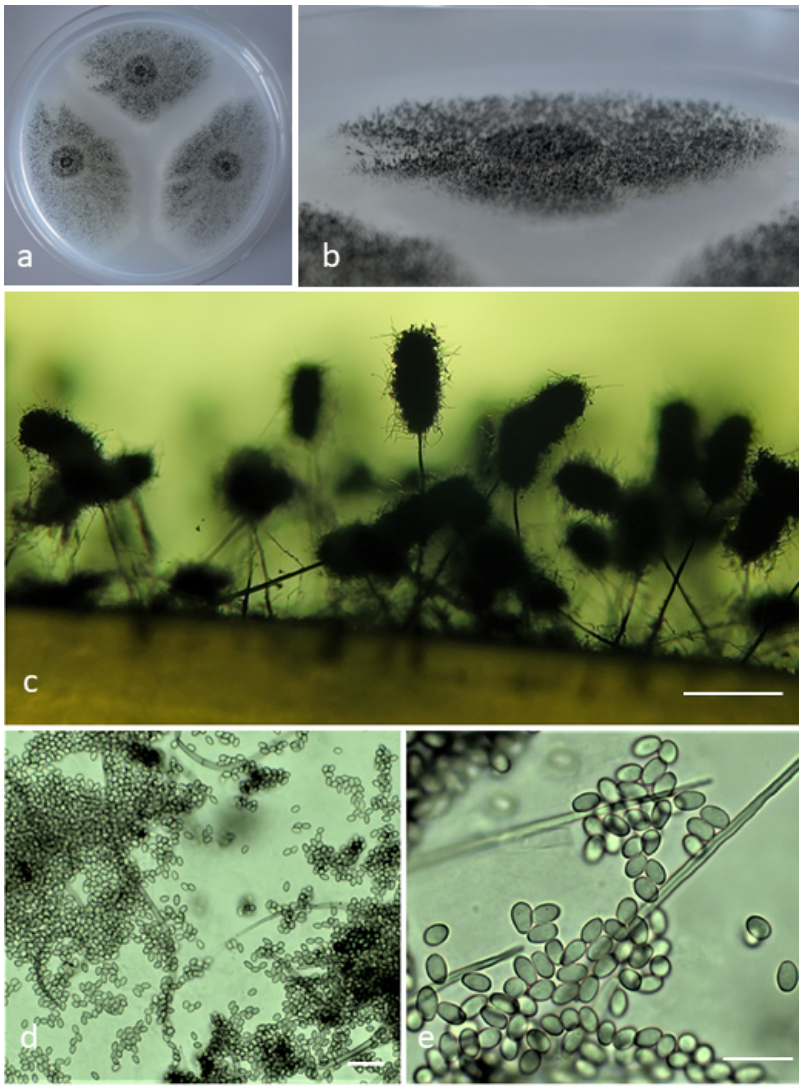

Figure 2

Cephalotrichum gorgonifer NG_p51. a-b. Colonies on OA after 14 d at 25°C (Petri dish = 9 cm diam). c. Synnemata in situ. d-e. setae and conidia. Scale bars: c = 200 µm, d = 20 µm, e = 10 µm

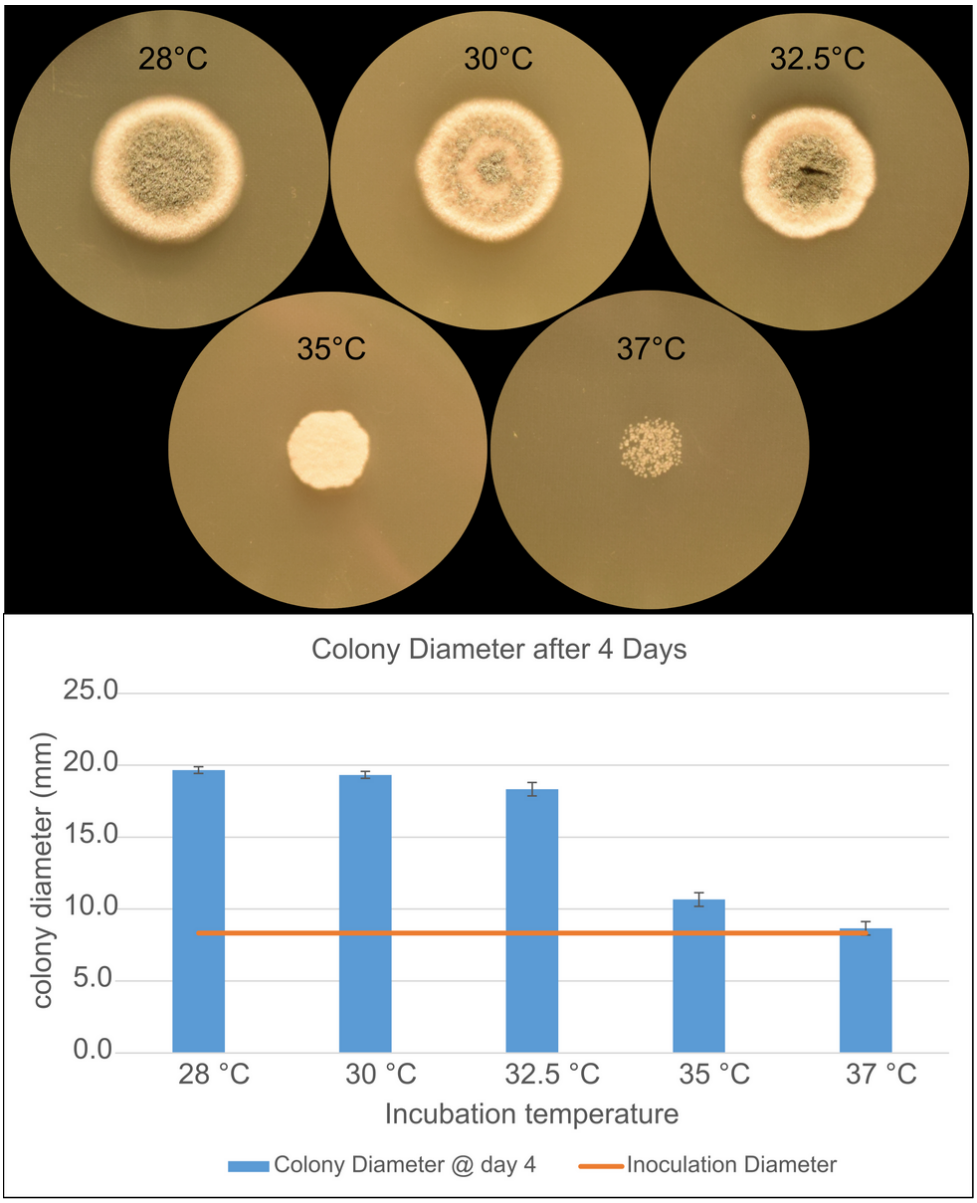

Figure 3

Radial growth of C. gorgonifer NG_p51 on MEA petri dishes at different 5 temperatures after 4 days.

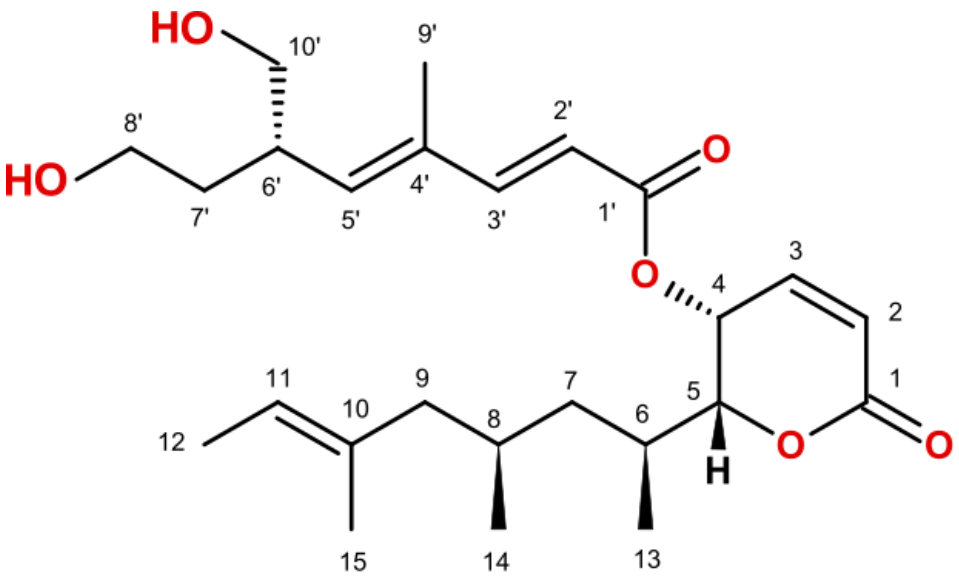

Figure 4

Structure of rasfonin

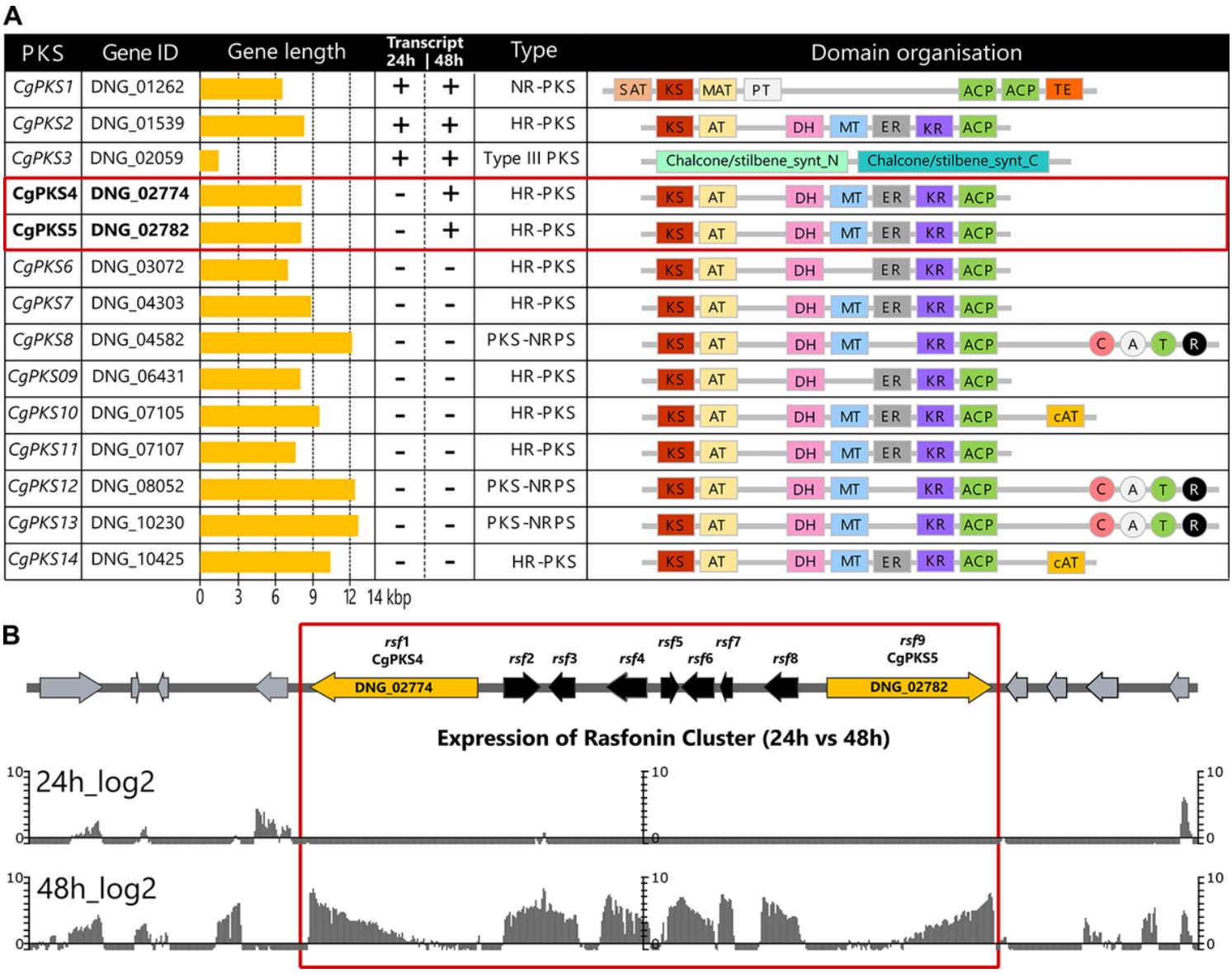

Figure 5

A Domain organization was analysed using the NCBI Conserved Domain (36), InterPro (37), SBSPKSv2 (38); and the PKS/NRPS Analysis Web-site (39). KS (red), keto synthase; AT (yellow), acyltransferase; DH (pink), dehydratase; MT (blue) C-methyltransferase; ER (grey) enoylreductase; KR (violet), ketoreductase; ACP (green), acyl carrier protein; cAT (orange), carnitine acyltransferase; Chalcone/stilbene_synt_N (lime-green): Chalcone/stilbene synthase N-terminal; Chalcone/stilbene_synt_C (dark-cyan): Chalcone/stilbene synthase C-terminal. The proposed PKS names are listed together with their gene number and length. The transcriptional activity at 24h or 48 hours ins indicated as "-" (No transcription at given timepoint) or "+" (transcription at given timepoint). The two PKS encoding genes that are proposed to be involved in the rasfonin synthesis (i.e. CgPKS4 and CgPKS5) are highlighted by a red box **B** The proposed BGC for rasfonin biosynthesis is depicted with transcript at 24h and 48h timepoint (shake flask culture, AMM). The BGC borders are depicted in red and were assigned based on the coregulation of genes. Proposed BGC gene names (rsf1 to rsf9) are depicted above gene illustrations.

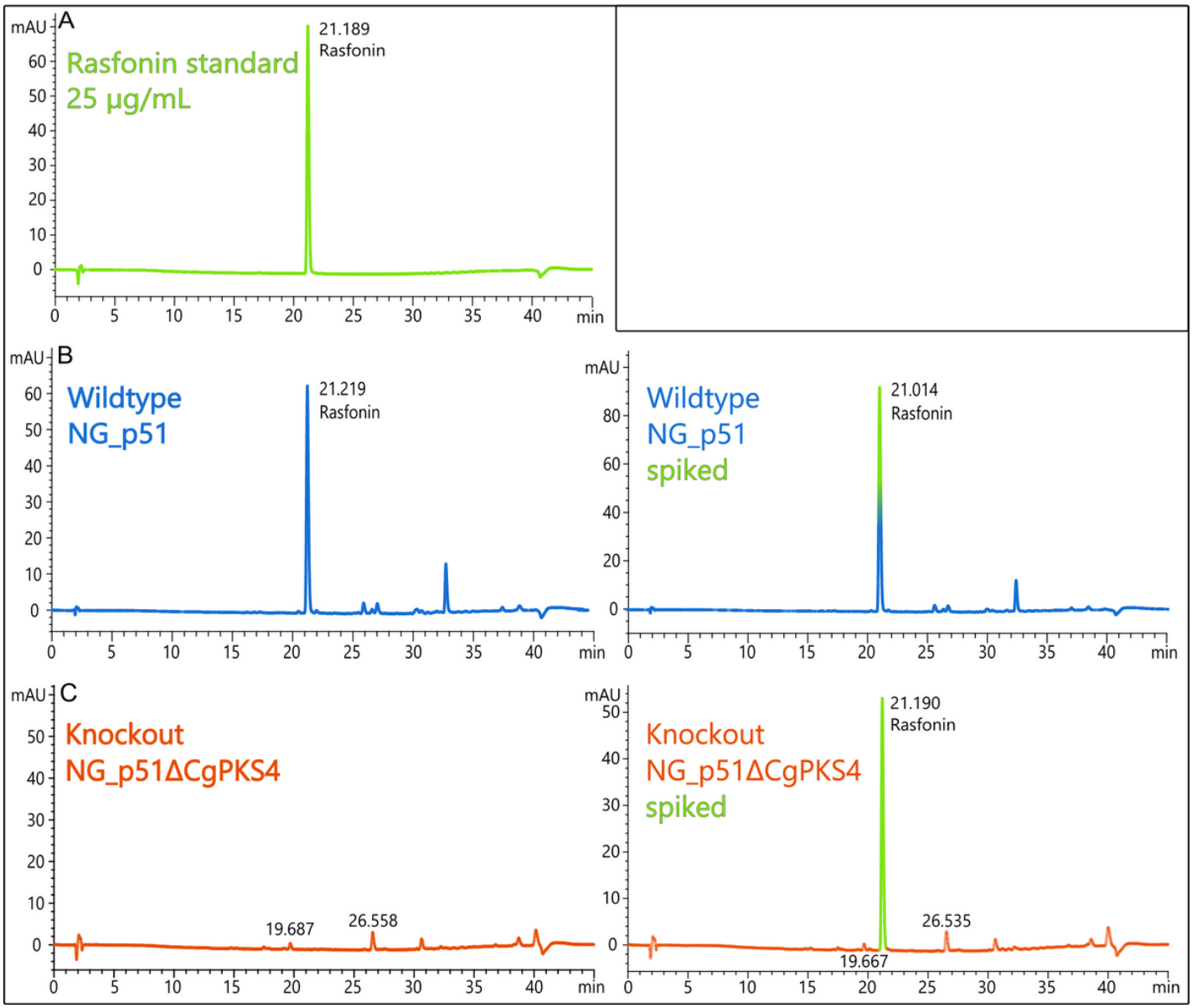

Figure 6

HPLC analysis of rasfonin between a 25 µg/mL rasfonin standard (green, **A**), the wildtype isolate NG_p51 (blue, **B left**) and the CgPKS4 knockout strain NG_p51ΔCgPKS4 (orange, **C left**). All 3 knockout strains and all replicates showed the same absence of rasfonin, but only one is shown here. Spiked samples are shown on the right panel and are indicated by a green peak (NG_p51, **B right**; NG_p51ΔCgPKS4, **C right**). The retention times in minutes are shown next to the peaks.

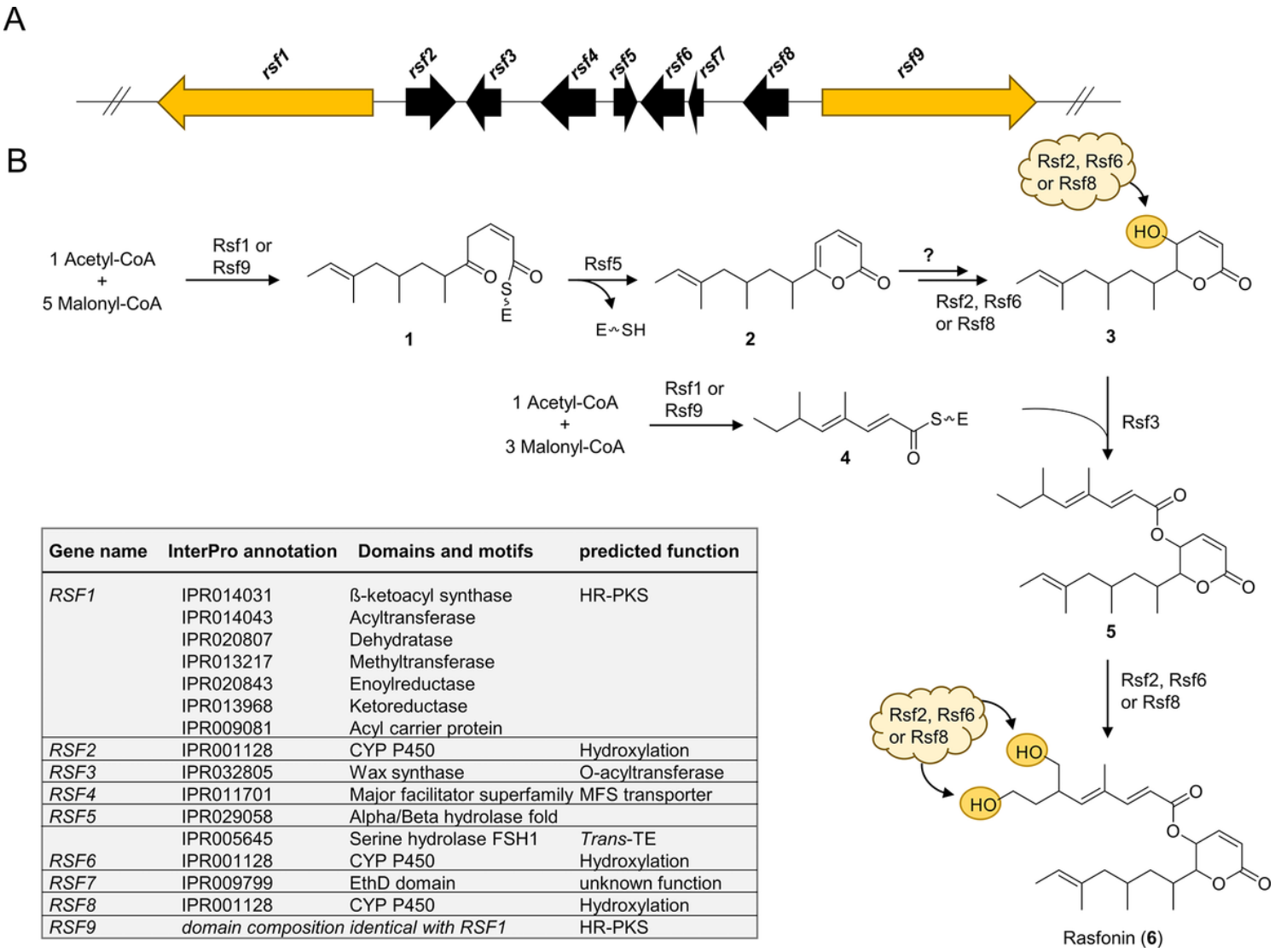

Gene name	InterPro annotation	Domains and motifs	predicted function
RSF1	IPR014031	ß-ketoacyl synthase	HR-PKS
	IPR014043	Acyltransferase	
	IPR020807	Dehydratase	
	IPR013217	Methyltransferase	
	IPR020843	Enoylreductase	
	IPR013968	Ketoreductase	
	IPR009081	Acyl carrier protein	
RSF2	IPR001128	CYP P450	Hydroxylation
RSF3	IPR032805	Wax synthase	O-acyltransferase
RSF4	IPR011701	Major facilitator superfamily	MFS transporter
RSF5	IPR029058	Alpha/Beta hydrolase fold	
	IPR005645	Serine hydrolase FSH1	*Trans*-TE
RSF6	IPR001128	CYP P450	Hydroxylation
RSF7	IPR009799	EthD domain	unknown function
RSF8	IPR001128	CYP P450	Hydroxylation
RSF9	*domain composition identical with RSF1*		HR-PKS

Figure 7

Proposed biosynthetic pathway of rasfonin. **A** The rasfonin BGC. **B** The proposed pathway of rasfonin synthesis

Supplementary Files

This is a list of supplementary files associated with this preprint. Click to download.

- Additionalfile1.pdf
- Additionalfile2.xlsx
- Additionalfile3.gbk
- Additionalfile4.gbk
- Additionalfile5.gbk
- Additionalfile6.gbk
- Additionalfile7.gbk